RESEARCH ARTICLE

The Raf-like MAPKKK INTEGRIN-LINKED KINASE 5 regulates purinergic receptor-mediated innate immunity in Arabidopsis

Daewon Kim[1], Dongqin Chen[1,3], Nagib Ahsan[2,4,5], Gabriel Lemes Jorge[2], Jay J. Thelen[2] and Gary Stacey[1,2,*]

[1]Division of Plant Science and Technology, C.S. Bond Life Science Center, University of Missouri, Columbia, MO 65211 USA
[2]Division of Biochemistry, C.S. Bond Life Science Center, University of Missouri, Columbia, MO 65211 USA
[3]Present Address: State Key Laboratory of Agrobiotechnology, College of Plant Protection, China Agricultural University, Beijing, 100193 China
[4]Present Address: Department of Chemistry and Biochemistry, The University of Oklahoma, Norman, OK 73019, USA
[5]Present Address: Mass Spectrometry, Proteomics and Metabolomics Core Facility, Stephenson Life Sciences Research Center, University of Oklahoma, Norman, OK, USA

***Author for correspondence:** staceyg@missouri.edu (G.S.)

Short title: Role of ILK5 in purinergic signaling cascades

The author(s) responsible for distribution of materials integral to the findings presented in this article in accordance with the policy described in the Instructions for Authors (https://academic.oup.com/plcell/pages/General-Instructions) is: Gary Stacey (staceyg@missouri.edu).

Abstract

Mitogen-activated protein (MAP) kinase signaling cascades play important roles in eukaryotic defense against various pathogens. Activation of the extracellular ATP (eATP) receptor P2K1 triggers MAP kinase 3 and 6 (MPK3/6) phosphorylation, which leads to an elevated plant defense response. However, the mechanism by which P2K1 activates the MAPK cascade is unclear. In this study, we show that in *Arabidopsis thaliana*, P2K1 phosphorylates the Raf-like MAP kinase kinase kinase (MAPKKK) INTEGRIN-LINKED KINASE 5 (ILK5) on serine 192 in the presence of eATP. The interaction between P2K1 and ILK5 was confirmed both *in vitro* and *in planta* and their interaction was enhanced by ATP treatment. Similar to *P2K1* expression, *ILK5* expression levels were highly induced by treatment with ATP, flg22, *Pseudomonas syringae* pv. *tomato* DC3000, and various abiotic stresses. ILK5 interacts with and phosphorylates the MAP kinase kinase MKK5. Moreover, phosphorylation of MPK3/6 was significantly reduced upon ATP treatment in *ilk5* mutant plants, relative to wild-type. The *ilk5* mutant plants showed higher susceptibility to *P. syringae* pathogen infection relative to wild-type plants. Plants expressing only the mutant ILK5^{S192A} protein, with decreased kinase activity, did not activate the MAPK cascade upon ATP addition. These results suggest that eATP activation of P2K1 results in transphosphorylation of the Raf-like MAPKKK ILK5, which subsequently triggers the MAPK cascade, culminating in activation of MPK3/6 associated with an elevated innate immune response.

Keywords

Mitogen-activated protein (MAP) kinase, Extracellular ATP, Integrin-linked kinase, ILK5, Purinergic signaling, P2K1, plant innate immunity

IN A NUTSHELL

Background: Extracellular ATP acts as a signaling molecule that is perceived by eukaryotic P2-type purinergic receptors, which are located in the plasma membrane. Purinergic signaling has been extensively studied in animals, including humans, but is less studied in plants. Pathogen invasion and subsequent wound stress releases extracellular ATP, a danger-associated molecular pattern (DAMP) signal, inducing purinergic signaling cascades, which result in phosphorylation of mitogen-activated protein kinases (MAPKs). Previous studies revealed that the P2K1 purinergic receptor increases MPK3/6 phosphorylation in response to eATP mediated purinergic signaling cascades in Arabidopsis.

Question: How does eATP recognition result in the activation of the MAP kinase cascade, which is essential for induction of the innate immune response in Arabidopsis plants?

Findings: The Raf-like MAPKKK INTEGRIN-LINKED KINASE 5 (ILK5) was shown to be a downstream substrate of P2K1 kinase activity. Initiation of an eATP-dependent signaling pathway by phosphorylation of ILK5 results in phosphorylation and activation of MKK5 leading to phosphorylation of MPK3/6 and downstream events crucial to the plant innate immune response.

Next steps: The discovery that release of eATP by pathogen invasion regulates MPK3/6 activation through phosphorylation of ILK5 provides information on DAMP signaling and pathogen resistance in plants. Future studies should aim to identify the plant mechanisms targeted by ILK5-mediated purinergic signaling cascades and use this knowledge to protect crops from the deleterious effects of a wide range of pathogens.

Introduction

Adenosine 5′-triphosphate (ATP) serves as an intracellular energy currency for all organisms. However, in both plants and animals, extracellular ATP (eATP) also functions as a danger-associated molecular pattern (DAMP) signal molecule when perceived by plasma-membrane localized purinoreceptors (Cao et al., 2014; Le et al., 2019). Mammals possess two major classes of purinoreceptors, ligand-gated ion channel P2X and G protein-coupled receptor P2Y, which have been extensively studied (Faria et al., 2012). eATP has been shown to play a variety of roles in mammals, including regulating immune response, inflammation, neurotransmission, muscle contraction, and cell death (Ferrari et al., 2016; Matzinger, 2007;

Cekic and Linden, 2016). In contrast to animals, the functional role of eATP in plants is not well studied. Nevertheless, published data suggests diverse roles for purinergic signaling in plants, including involvement in response to biotic and abiotic stresses (Song et al., 2006; Chen et al., 2017; Deng et al., 2015; Thomas et al., 2000), gravitropism (Tang et al., 2003), root hair growth (Kim et al., 2006; Lew and Dearnaley, 2000), root avoidance (Zhu et al., 2017), thigmotropism (Weerasinghe et al., 2009), and cell death (Chivasa et al., 2005; Feng et al., 2015).

Plants lack canonical P2X and P2Y receptors (Choi et al., 2014a, 2014b). Thus, it was a significant breakthrough when the first plant purinergic receptor was identified as a member of the lectin receptor-like kinase family (i.e., LecRK I.9), originally termed DOESN'T RESPOND TO NUCLEOTIDES 1 (DORN1) but more recently named P2K1, in keeping with the nomenclature originally established in animals for P2-type purinoreceptors (Choi et al., 2014a; Chen et al., 2017). P2K1/DORN1 (LecRK I.9) was originally identified as a positive regulator of plant defense against the oomycete pathogens, *Phytophthora brassicae* and *Phytophthora infestans*, and the bacterial pathogen *Pseudomonas syringae* pv. *tomato* DC3000 (*Pst* DC3000) (Chen et al., 2017; Bouwmeester et al., 2011; Balagué et al., 2017; Bouwmeester et al., 2014; Wang et al., 2016). However, the primary biochemical function of P2K1 appears to be as a receptor during developmental and stress conditions that induce the release of eATP (e.g., upon wounding) (Choi et al., 2014b; Cao et al., 2014).

Recently, it was demonstrated that P2K1 plays an important role in regulating the production of reactive oxygen species (ROS) via direct phosphorylation of NADPH oxidase (i.e., RBOHD) regulating both stomatal aperture and eATP mediated danger-associated molecular pattern-triggered immunity (Chen et al., 2017). Indeed, very recently it was shown that eATP triggers a ROS wave in plants that is dependent on P2K1 function (Myers et al., 2022). It was also shown that S-acylation affects the temporal dynamics of P2K1 receptor activity through autophosphorylation and protein degradation (Chen et al., 2021). The CYCLIC NUCLEOTIDE GATED CHANNEL 6 (CNGC6) and CNGC2 proteins were shown to play a crucial role in mediating eATP-induced cytosolic Ca^{2+} signaling (Chen et al., 2021; Duong et al., 2021; Wang et al., 2022). Animals possess multiple P2X and P2Y receptors and, hence, it was perhaps no surprise when a second plant purinoreceptor, P2K2 (LecRK I.5), was identified (Pham et al., 2020). Both P2K1 and P2K2 bind ATP and ADP with high affinity to activate a plant pattern-triggered immune response (Choi et al., 2014a; Pham et al., 2020). Among the various downstream events activated by eATP is

phosphorylation of MAP kinase 3 and 6, which is markedly reduced in *p2k1 p2k2* double mutant plants (Choi et al., 2014a; Pham et al., 2020).

The mitogen-activated protein kinase (MAPK) cascade plays a critical role in transmitting and amplifying stimulus-specific signals to the cellular machinery by phosphorylation of target proteins in eukaryotes (Cristina et al., 2010; Thulasi Devendrakumar et al., 2018). Compared to the small number of plant MAPKK and MAPK family members, MAPKKKs constitute a larger family, which are considered essential to the ability to respond to diverse signals/environmental conditions (MAPK Group, 2002; Cristina et al., 2010). For example, the *Arabidopsis thaliana* genome encodes genes for 20 MAPK, 10 MAPKK and 80 MAPKKK subfamily members (MAPK Group, 2002; Cristina et al., 2010). Plant MAPKKK are divided into three subfamilies, MEKK, Raf, and ZIK, which consist of 21, 48, and 11 members, respectively. Among the Raf-like MAPKKK members, ENHANCED DISEASE RESISTANCE 1 (EDR1/Raf2) and CONSTITUTIVE TRIPLE RESPONSE 1 (CTR1/Raf1) are relatively well characterized (Frye and Innes, 1998; Frye et al., 2001). CTR1 encodes a serine/threonine kinase that negatively regulates ethylene signaling by acting upstream of MKK9 and MPK3/6 (Kieber et al., 1993; Clark et al., 1998; Yoo et al., 2008). Another Raf-like MAPKKK, EDR1 regulates MAPK cascades via direct association with MKK4/MKK5 for negative regulation of salicylic acid (SA)-inducible plant defense responses (Frye et al., 2001).

Integrin-linked Kinases (ILKs), a Raf MAPKKK subfamily with unique characteristics, are thought to play an important role in diverse biological functions in plants (Popescu et al., 2017). The first ILK described was shown to be an interacting partner of the integrin receptor cytoplasmic β subunit, functioning in the assembly of signaling complexes at plasma membrane focal adhesion regions in metazoans (Hannigan et al., 1996; Tu et al., 2001). ILKs were originally characterized as serine/threonine kinases, but recent studies have questioned whether ILKs actually function as kinases (Hannigan et al., 2011; Dagnino, 2011). Instead, ILKs were proposed to function as scaffolding proteins with adaptor proteins, PINCH and α-parvin (IPP complex), to regulate various biological processes, such as cell adhesion, migration, proliferation, differentiation, assembly of the extracellular matrix (ECM) and contractility (Hannigan et al., 1996; Tu et al., 2001; Dagnino, 2011; Hannigan et al., 2011; Meder et al., 2011). In contrast to metazoans, plant genomes encode multiple ILK genes [e.g., ILK1-6 in Arabidopsis] (Popescu et al., 2017). Plant ILKs were first described as N-terminus ankyrin repeat containing kinases

suggested to play a role in osmotic stress and adventitious root growth in *Medicago truncatula* and Arabidopsis (Chinchilla et al., 2008, 2003). Recently, ILK1 was demonstrated to modulate the sensitivity of plants to osmotic and saline stress, response to nutrient availability, and response to bacterial pathogens (Brauer et al., 2016; Popescu et al., 2017). While metazoan ILKs have been studied intensively, their role in molecular signaling in plants is poorly understood (Popescu et al., 2017).

In this study, we identified Raf-like MAPKKK ILK5/Raf27/BHP (BLUE LIGHT-DEPENDENT H^+-ATPASE PHOSPHORYLATION; hereafter referred to as ILK5), previously characterized as a regulator of blue light-dependent stomatal movement (Hayashi et al., 2017), as a protein substrate of the P2K1 kinase in pattern-triggered immunity. Indeed, P2K1 directly phosphorylates ILK5 on Ser192. Interaction between P2K1 and ILK5 was confirmed using a variety of *in vitro* and *in vivo* methods. Here, we reveal that the presence of an eATP-dependent signaling activation initiated by phosphorylation of ILK5 with subsequent activation of MKK5, leading to activation of MPK3/6 and downstream events crucial to the plant innate immune responses.

Results

Raf-like MAPKKK ILK5 is Phosphorylated by P2K1

In order to identify substrate proteins for the P2K1 kinase domain, a mass spectrometry-based *in vitro* phosphorylation strategy, termed kinase client (KiC) assay (Ahsan et al., 2013; Huang et al., 2010), was used. A synthetic peptide library representing approximately 2100 experimentally identified *in vivo* phosphorylation sites was incubated with GST-fused P2K1 cytosolic domain recombinant protein (GST-P2K1-CD) in the presence of ATP. Subsequently, tandem mass spectrometry was performed to identify both phospho-peptides and specific phosphorylation sites. The result of this experiment was the identification of twenty-three phosphorylated peptides, which were identified and verified by phosphoRS score and phosphoRS site probability. As previously published, three protein substrates identified from this screen were RESPIRATORY BURST OXIDASE HOMOLOG D (RBOHD) and PROTEIN S-ACYLTRANSFERASE 5/9 (PAT5/9), which were subsequently shown to be regulated by P2K1 phosphorylation (Chen et al., 2017, 2021). In this study, the VKKLDDEVLS(p)^{192} peptide of ILK5 was phosphorylated by the P2K1 kinase domain (Figure 1A). According to the BLAST search and Pfam

database, ILK5 has the typical Raf-like MAPK kinase kinase (MAPKKK) structure with a N-terminal ankyrin-repeat domain and C-terminal Ser/Thr kinase domain.

It was previously reported that P2K1 has strong kinase activity, which is essential for eATP-induced MPK3/6 phosphorylation *in planta* (Choi et al., 2014a; Cho et al., 2022). To investigate phosphorylation of ILK5 MAPKKK protein upon eATP treatment *in vivo*, ILK5-HA protein was expressed in Arabidopsis protoplasts and subsequently immunoprecipitated with an anti-HA antibody bead, then probed by immunoblotting with an anti-phospho-Ser/Thr antibody. Significantly increased ILK5 phosphorylation was detected under ATPγS (poorly hydrolyzed ATP analog) treatment (Figure 1B). In order to confirm the results of the KiC assay, purified recombinant ILK5 protein was incubated with either purified GST-P2K1-CD, kinase dead version of P2K1 (GST-P2K1^{D572N}-CD or GST-P2K1^{D525N}-CD) in the presence of [γ-^{32}P] ATP. The results of this assay showed that GST-P2K1-CD directly trans-phosphorylated ILK5-His and the generic substrate MBP, but not CPK5^{D221A} protein used as a negative control. Assays performed with the two kinase-dead versions of P2K1 failed to phosphorylate ILK5-His (Figure 1C). To verify that the radiography signal was the result of phosphorylation, the addition of lambda protein phosphatase (Lambda PPase) was shown to reduce both auto- and trans-phosphorylation of P2K1 and ILK5 (Supplemental Figure S1A). The tandem MS results from the KiC assay revealed Ser192 residue of ILK5 was the specific target of P2K1 phosphorylation. To confirm this, site-directed mutagenesis was used to generate an ILK5^{S192A} recombinant protein, which was purified and incubated with purified GST-P2K1-CD. As expected, the results showed a significant reduction in phosphorylation of ILK5^{S192A} recombinant protein, relative to the wild-type protein (Figure 1, D and E; Supplemental Figure S1B).

To demonstrate whether Ser192 of ILK5 is an *in vivo* target residue of P2K1, ILK5-HA or ILK5^{S192A}-HA protein was expressed in Arabidopsis protoplasts and subsequently immunoprecipitated with an anti-HA antibody bead then probed by immunoblotting with an anti-phospho-Ser/Thr antibody. Mutation of ILK5 at the Ser192 residue (ILK5^{S192A}) led to significantly reduced phosphorylation by P2K1 (Figure 1F). To investigate whether ILK5 phosphorylation is dependent on P2K1, ILK5-HA protein was expressed in wild-type, *p2k1-3* and *P2K1*-overexpressing plants (*OXP2K1*) under ATPγS treatment followed by immunoprecipitation using anti-HA antibody. Immunoblotting was subsequently performed with an anti phospho-Ser/Thr antibody. Reduction of phosphorylation and increased phosphorylation in ILK5-HA protein was detected in *p2k1-3* and *OXP2K1* compared to wild-type, respectively (Figure 1G).

These results indicate that ILK5 is phosphorylated by P2K1 kinase, and that the ILK5 Ser192 residue is the major target of this phosphorylation event.

P2K1 interacts with ILK5

In previous reports, P2K1 was localized to the plasma membrane (Bouwmeester et al., 2011), while ILK5 was predicted to localize in the cytosol (SUBA; http://suba.plantenergy.uwa.edu.au) (Hayashi et al., 2017). In order to confirm the subcellular localization of ILK5 in Arabidopsis, a YFP (C-terminus or N-terminus) tagged ILK5 was expressed in Arabidopsis plants and protoplasts. The bulk of ILK5 co-localized with the FM4-64 (plasma membrane marker) in Arabidopsis transgenic plants and protoplasts (Figure 2A; Supplemental Figure S2).

Phosphorylation of ILK5 by P2K1 is consistent with direct interaction between these two proteins. To provide further evidence for this interaction, we co-expressed HA-tagged P2K1 with a Myc-tagged ILK5 in *Nicotiana benthamiana* leaves in the presence and absence of exogenous eATP, followed by immunoprecipitation using antibodies to the specific epitope tags. Consistent with a direct interaction, P2K1 and ILK5 were co-immunoprecipitated and their interaction appeared to be enhanced in the presence of eATP (Figure 2B). We further confirmed these results using split-luciferase complementation imaging (LCI) (Figure 2, C and D; Supplemental Figure S3 and S4A). Bimolecular fluorescence complementation (BiFC) assays were conducted in Arabidopsis protoplasts in order to demonstrate the interaction of P2K1 with ILK5 at the plasma membrane. Co-expression of P2K1-nYFP with ILK5-cYFP produced a yellow fluorescent signal that co-localized with the plasma membrane marker FM4-64, whereas co-expression of P2K1-nYFP with the control ILK6-cYFP protein did not display a yellow fluorescent signal (Figure 2E; Supplemental Figure S4B). Hence, the data are consistent with a direct interaction of P2K1 and ILK5 at the plasma membrane.

ILK5 has kinase activity and activates MKK5

ILKs are involved in various processes in animals; however, kinase activity is not essential to the regulation of these processes (Wu and Dedhar, 2001; Hannigan et al., 2011). Indeed, there is some dispute whether animal ILKs possess kinase activity (Hannigan et al., 2011). However, in contrast to the animal situation, an examination of plant ILK protein sequences suggests that the core residues necessary for

kinase activity are well conserved (Popescu et al., 2017). These results suggest that ILK5, found in the Group C cluster of the Raf-like subfamily, may possess kinase activity (Popescu et al., 2017). However, a previous study (Hayashi et al., 2017), as well as our own efforts, failed to find ILK5 kinase activity using protein purified after expression in bacterial cells (Supplemental Figure S5A). Interestingly, in contrast to protein expressed in bacteria, a previous study showed that ILK1 protein extracted from plant tissue had true kinase activity (Brauer et al., 2016). Therefore, we expressed and purified the N-terminally tagged His-tag in frame ILK5 (His-ILK5) and GFP protein (His-GFP) from *N. benthamiana* leaves. The ILK5 protein purified in this way was able to auto- and trans-phosphorylate MBP, but not His-GFP protein (Supplemental Figure S5, B-D). It was verified by mass spectrometry that the result was not caused by contamination with other kinases (Supplemental Data Set 1). In addition, when the key residue K184 was substituted with alanine (His-ILK5^{K184A}), most of the auto- and trans-phosphorylation activities of ILK5 disappeared (Supplemental Figure S6A).

To determine if phosphorylation of ILK5 at S192 is required for kinase activity, *in vitro* kinase assays using phosphor-null (S192A) and phosphor-mimic (S192D) mutants were carried out. It was observed that S192A version of the ILK5 dramatically reduced kinase activity while the S192D mutation slightly increased kinase activity compared to WT ILK5 protein (Supplemental Figure S6B). Taken together, we can conclude that ILK5 is an active kinase. These results are also consistent with the previous report that ILK5 protein expressed and purified from wheat germ cells possessed kinase activity (Nemoto et al., 2011).

If ILK5 acts as a MAPKKK, one would expect it to interact with and activate downstream MAPK kinases. We investigated the interaction of ILK5 with MKK5 by BiFC analysis. MKK5 was chosen since it was previously shown to regulate phosphorylation of MPK3/6 and, hence, play an essential role in regulating the plant immune response (Asai et al., 2002; Popescu et al., 2009). YFP signals were observed mainly in the cytoplasm and some nuclei of plants carrying MKK5-nYFP and ILK5-cYFP indicating that interactions between ILK5 and MKK5 took place in the cytoplasm and nucleus (Figure 3A and Supplemental Figure S7A). These physical protein-protein interactions were confirmed by a GST-pull-down assay using ILK5 protein derived from *N. benthamiana*. His-GFP protein was used as a negative control (Figure 3B).

To further investigate this interaction under ATP treatment, we co-expressed MKK5-nLUC with ILK5-cLUC and monitored luciferase intensity in the presence and absence of exogenous eATP. Leaves treated with ATP showed markedly increased MKK5-ILK5 protein interaction (Figure 3, C and D; Supplemental Figure S7B). Furthermore, in order to examine whether ILK5 directly phosphorylates MKK5, *in vitro* kinase assays were performed with His-tagged ILK5 extracted from *N. benthamiana* plants and GST-His-tagged MKK4 and MKK5. In previous reports, MKK4 and MKK5 were shown to have strong auto- and trans-phosphorylation activities (Yamada et al., 2016). Therefore, kinase dead versions of MKK4 ($MKK4^{K108R}$) and MKK5 ($MKK5^{K99R}$) were generated by site-directed mutagenesis according to a previous study (Yamada et al., 2016) (Supplemental Figure S7C). The results showed that ILK5 directly phosphorylates $MKK5^{K99R}$, while phosphorylation of $MKK4^{K108R}$ was not detectable. (Figure 3E). According to the results of the KiC assay and phosphorylation assay, Ser192 of ILK5 was identified and confirmed as a target key residue of the P2K1 kinase (Figure 1). Interestingly, phosphorylation of $MKK5^{K99R}$ protein was significantly reduced when incubated with the $ILK5^{S192A}$ phosphor-null protein (Figure 3E).

Previously, it was shown that MKK5 phosphorylation of Thr215 and Ser221 in the activation loop is required for MPK3/6 activation (Yamada et al., 2016). To determine whether these two key residues of the MKK5 are phosphorylated by ILK5, GST-$MKK5^{K99RT215AS221A}$ was generated using site-directed mutagenesis. As shown in Figure 3F, significantly reduced phosphorylation of GST-His-$MKK5^{K99RT215AS221A}$ was detected compared with GST-His-$MKK5^{K99R}$ (Figure 3F). To further investigate whether MKK5 phosphorylation is dependent on the ILK5 protein *in vivo*, MKK5-HA protein was expressed in wild-type and *ilk5-1* protoplasts under ATP treatment followed by immunoprecipitation using an anti-HA antibody and subsequent immunoblotting with an anti-phospho-Ser/Thr antibody. Phosphorylation in MKK5-HA was significantly reduced in *ilk5-1* compared to wild-type in the presence of exogenous ATP (Figure 3G).

ILK5 is highly induced by ATP, pathogen and wounding, similar to *P2K1*

Published work documents that eATP is released from plant cells in response to various stresses (e.g., pathogen infection), as well as wounding (Cao et al., 2014; Chen et al., 2017; Myers et al., 2022). In order to investigate the expression patterns of *ILK5* under comparable stress conditions, we stably transformed

either a *ILK5promoter:GUS* or *ILK5promoter:GFP* construct into Arabidopsis. A published study indicated that *ILK5* is highly expressed in guard cells (Hayashi et al., 2017). Consistent with this published work, our *ILK5promoter:GUS* and *GFP* transgenic plants showed strong expression in guard cells (Figure 4A; Supplemental Figure S8A). The GUS signals observed in *ILK5promoter:GUS* and *P2K1promoter:GUS* (Choi, 2013) transgenic plants showed ubiquitous expression in various tissues, including rosette leaves, primary roots, and cotyledons under normal growth conditions (Supplemental Figure S8B). Subsequently, RT-qPCR was use to confirm expression of both *ILK5* and *P2K1* expression in various tissues (Supplemental Figure S8C).

Previous published work clearly showed a critical role for P2K1 in mediating the plant defense response to various pathogens, as well as pathogen associated responses, including jasmonate signaling (Balagué et al., 2017; Wang et al., 2016; Tripathi et al., 2018). In order to investigate whether *ILK5* is highly induced by such treatments including pathogen and ATP treatments, GUS activity was observed in response to various treatments in transgenic plants expressing the *ILK5promoter:GUS* construct. GUS activity driven by an *ILK5* promoter was strongly up-regulated by treatment with the pathogen *P. syringae* DC3000, the pathogen-associated molecular pattern (PAMP) flagellin peptide flg22, MeJA, wounding and eATP relative to mock treatments (Figure 4A, D and G). These results were confirmed by RT-qPCR analysis using RNA extracted from the treated plants (Figure 4, B, C, E and F). Similar results were obtained by immunoblot quantification of *ILK5promoter:GFP* expression using an anti-GFP antibody and protein from plants treated with either *P. syringae* DC3000 or eATP over a time course (Supplemental Figure S8, D and E). These results support the notion that both *ILK5* and *P2K1* expression responds to a variety of stresses, consistent with their coordinated role in regulating purinergic signaling initiated by the release of eATP in response to stress.

ILK5 plays an important role in the pathogen defense response

According to previous studies, extracellular ATP (eATP) regulates the MAPK pathway through phosphorylation in both plants and mammals (Neary et al., 1999; Choi et al., 2014a; Pham et al., 2020). To confirm this, we examined the phosphorylation of MPK3/6 in the wild-type and *p2k1* mutants upon treatment with ATP over a time course (Supplemental Figure S9). The results showed that *p2k1-1* (D572N), *p2k1-2* (D525N), and *p2k1-3* (Salk-042209) mutants showed significantly reduced phosphorylation of

MPK3/6 compared to wild-type (Supplemental Figure S9B). Conversely, phosphorylation of MPK3/6 was significantly increased in transgenic plants ectopically over-expressing P2K1 (*OXP2K1*) (Supplemental Figure 9C).

To demonstrate the specificity of MPK3/6 phosphorylation in *p2k1-3* and *OXP2K1*, various elicitors such as flg22, chitin, elf26, and pep1 were applied. However, the *p2k1-3* and *OXP2K1* appeared to have no effect on MPK3/6 in response to these elicitors (Supplemental Figure S10). P2K1 presumably transmits purinergic signaling via ATP-induced phosphorylation of downstream target proteins to activate the MAPK pathway.

The gene expression patterns and biochemical data presented above suggest that defects in ILK5 function should disrupt the normal response to pathogen infection. To examine this directly, we conducted functional analysis using *ilk5* T-DNA insertion mutants (Supplemental Figure S11). *ilk5-2* and *ilk5-4* showed low gene expression or minor change, likely due to insertion of the T-DNA in either 5'-UTR or 3'-UTR (Supplemental Figure S11, C and D). In contrast, *ILK5* transcripts were not detected in *ilk5-1* and *ilk5-3* mutants, suggesting that *ilk5-1* and *ilk5-3* are null alleles (Supplemental Figure S11, C and D).

In order to understand how ILK5 is involved in MPK3/6 phosphorylation under ATP treatment, phosphorylation of MPK3/6 was examined after ATP treatment. Phosphorylation of MPK3/6 was significantly reduced in both *ilk5-1* and *ilk5-3* mutants (Figure 5A). To demonstrate the specificity of MPK3/6 phosphorylation in *ilk5* mutants, plants were treated with various elicitors such as flg22, chitin, elf26, and pep1 and then analyzed via immunoblotting using α-p44/42 antibody. Although phosphorylation of MPK3/6 in *ilk5* mutants slightly decreased after 30 min when treated with elf26 and pep1, but overall, there was no significant difference compared to WT plants. (Supplemental Figure S12; A-D).

In a previous report, MAPKKK3 and MAPKKK5 were shown to regulate the phosphorylation of MPK3/6 by several PRRs and confer resistance to bacterial and fungal pathogens in *Arabidopsis thaliana* (Bi et al., 2018). Interestingly, the phosphorylation of MPK3/6 was reduced in the *mapkkk3 mapkkk5* double mutant under ATP treatment (Supplemental Figure S12E). Furthermore, pathogen defense-responsive genes such as *WRKY40* and *CPK28* transcripts were quantified by RT-qPCR under ATP treatment, with both transcripts being significantly reduced in *ilk5-1* and *ilk5-3* mutants (Figure 5B and C). These results imply that ILK5 positively regulates pathogen resistance and ATP-inducible defense

responses in Arabidopsis. Thus, disease resistance against the virulent pathogen, *luxCDABE*-tagged *P. syringae DC3000*, was examined with or without addition of ATP in *ilk5-1* and *ilk5-3* mutants. Consistent with our biochemical studies, the *ilk5-1* and *ilk5-3* mutant plants showed enhanced susceptibility to *P. syringae* infection (Figure 5, D-F).

Consistent with these results, phosphorylation of MPK3/6 was restored in complemented lines in which the wild-type *ILK5* was driven by the *ILK5* native promoter (Figure 6A; Supplemental Figure S13A). In addition, phosphorylation of MPK3/6 was also significantly reduced in *ilk5-1* plants expressing the ILK5^{S192A} protein (Figure 6B; Supplemental Figure S13B). Interestingly, we also found that *ilk5-1* plants expressing the ILK5^{S192A} mutant protein were significantly more susceptible to pathogen infection than wild-type (WT) or ILK5^{WT} complemented plants (Figure 6, C-E). These results show that ILK5^{S192A} complemented transgenic plants were more susceptible to pathogen infection and that the ILK5 Ser192 residue plays a critical role in MAPK pathway activation, which impacts the level of disease resistance.

To determine whether this reduction in phosphorylation of MPK3/6 was not caused by protein destabilization, immunoblotting was performed using anti-MPK3 or MPK6 antibodies under ATP treatment in *ilk5* mutants or transgenic plants expressing ILK5^{WT} or ILK5^{S192A} protein in the *ilk5-1* background. Significant reduction or increase in MPK3 or MPK6 protein was not detected under ATP treatment after 30 minutes, confirming the reduction of phosphorylation was not due to the protein destabilization (Supplemental Figure S14).

In previous studies, addition of ATP was shown to trigger stomatal closure and enhance innate immunity when plants were sprayed or dip inoculated with the pathogen (Chen et al., 2017; Clark et al., 2011). Hence, it is of interest that *ILK5* is highly expressed in guard cells and was previously shown to play a role in modulating stomatal aperture (Hayashi et al., 2017). Therefore, we examined the ability of the stomata to close in *ilk5-1* mutant plants upon ATP treatment. The movement of the stomata in *ilk5-1* mutant was mis-regulated (Supplemental Figure S15). This suggests that, similar to P2K1, ILK5 functions in regulating stomatal closure in response to eATP and, thereby, controls the ability of the bacterial pathogen to enter the leaf via stomata.

In summary, we hypothesize the following role for ILK5 in plant purinergic signaling. When a pathogen invades causing the release of eATP, the P2K1 receptor is activated by eATP recognition.

Subsequently, P2K1 directly interacts with and phosphorylates the downstream ILK5 kinase protein, leading to an innate immune response via activation of the MAPK cascades (Figure 7).

Discussion

Role of integrin-linked kinase in purinergic signaling

Extracellular ATP is a conserved danger-associated molecular pattern in eukaryotes and, hence, purinergic signaling plays a critical role in the ability of both animals and plants to response to stress (Le et al., 2019; Cekic and Linden, 2016; Salmaso and Jacobson, 2020). Integrins are heterodimeric cell membrane receptors composed of α and β subunits that mechanically function by binding the cell cytoskeleton to the extracellular matrix (ECM) (Hynes, 2002). Integrins regulate signal transduction pathways that mediate multiple cellular signals such as organization of cytoskeleton, regulation of the cell cycle, cell adhesion, migration, and activation of growth factor receptors (Hynes, 2002; Desgrosellier and Cheresh, 2010; Kim et al., 2011). Interestingly, integrin and purinergic signaling are closely regulated in metazoans. For example, the human $P2Y_2$ nucleotide receptor directly interacts with $\alpha_v\beta_3$ and $\alpha_v\beta_5$ integrin complexes via the integrin-binding domain, arginine-glycine-aspartic acid (RGD), contained in $P2Y_2R$ (Bagchi et al., 2005). The RGD sequence was also found to be essential for the role that $P2Y_2R$ plays in UTP-induced chemotaxis via G_0 protein coupling. Additionally, Bye et. al., reported that $\alpha_{IIb}\beta_3$ (GPIIb/IIIa) integrin protein is activated by $P2Y_1$-stimulated Ca^{2+} signaling and $P2Y_{12}$-stimulated activation of the PI3 kinase, which is essential for fibrinogen binding to the platelet of primary rat megakaryocytes (Bye et al., 2020).

Integrins and integrin-linked kinases in animals have been well characterized; however, homologs of animal integrins appear to be absent in plants (Knepper et al., 2011). As the name suggests, integrin-linked kinases strongly interact with the *β* subunits of integrin receptors mediating formation of signaling complexes that are localized at sites of plasma membrane-extracellular matrix interaction (i.e., focal adhesion zones) (Dagnino, 2011; Wu and Dedhar, 2001). It is also interesting that P2K1 (LecRK I.9) was reported to mediate plasma membrane-cell wall interaction (Bouwmeester et al., 2011). Hence, it is possible that in the absence of true integrins, plants might be regulating such receptors as a means to construct signaling complexes at sites of plasma membrane-cell wall adhesion.

Phosphorylation of MAPK in purinergic signaling

Activation of a MAPK cascade is a purinergic signaling response shared between animals and plants (Thevananther et al., 2004; Markou et al., 2003). For instance, $P2Y_2$ mediated cell growth is highly stimulated by eATP through MAPK/ERK kinase activation (Neary et al., 1999; Schultze-Mosgau et al., 2000). In addition, purinergic signaling activates cPLA2 by another downstream kinase, the mitogen- and stress-activated kinase-1 (MSK1), in order to simultaneously activate both the required ERK1/2 and p38 MAPK (Markou et al., 2003). Extracellular ATP induces animal cell cycle progression beyond the G1 phase of the cell cycle by activation of P2 receptors (Thevananther et al., 2004). When P2 receptors are activated, protein kinase C (PKC) transmits signals to the nucleus through one or more of the MAPK cascades, which possibly include Raf-1, MEK, and ERK, and stimulates transcription factors such as MYC, MAX, FOS, and JUN (Cekic and Linden, 2016; Thevananther et al., 2004).

Previous research showed that phosphorylation of MPK3/6 was activated in plants upon eATP addition and required P2K1 function, but was also reduced in the absence of P2K2 (Choi et al., 2014a; Pham et al., 2020). The current study provides this connection by presenting several lines of evidence consistent with the hypothesis that P2K1 activation leads to ILK5 activation, followed by MKK5 activation and then phosphorylation of MPK3/6, the latter as previously published (Asai et al., 2002). Although we found that the MAPKKK ILK5 is involved in MPK3/6 phosphorylation, MPK3/6 phosphorylation was not completely abolished in the *ilk5* mutants under ATP treated conditions (Figure 5A). In previous studies, several plant MAPKKKs were reported that regulate the phosphorylation of MPK3/6 in biological processes or environmental stress conditions, especially in innate immunity. For example, Arabidopsis MEKK1 (MEKK1–MKK4/MKK5–MPK3/MPK6) is involved in FLAGELLIN SENSITIVE2 **(**FLS2) mediated plant immune response (Asai et al., 2002) and MAPKKK3 and MAPKKK5, mediated MPK3/6 activation in response to activation of several pattern recognition receptors (PRRs) and receptor-like cytoplasmic kinases that play important roles in resistance to several fungal and bacterial diseases (Bi et al., 2018). PRRs recognize PAMPs and DAMPs, which then transmit the signals to MAPKKKs, where receptor-like cytoplasmic kinases are heavily involved (Liang and Zhou, 2018). Compared to the MEKK subfamily, Raf-like MAPKKKs are not well characterized in part due to the mutually complementary relationships between the Raf-subfamily of MAPKKK proteins. There are six ILK members in Arabidopsis, with ILK4 being the most similar in protein sequence to ILK5. In a recent report, ILK1 was shown to regulate MPK3/6 phosphorylation in response to treatment with the

flg22 peptide (Brauer et al., 2016). Interestingly, it was found that the phosphorylation of MPK3/6 was reduced upon ATP treatment in *mapkkk3 mapkkk5* double mutants (Supplemental Figure S12E). Therefore, ILK5 has the potential to function in a complementary relationship with another subgroup of MAPKKKs (i.e., MAPKKK3 and MAPKKK5) or other Raf-like MAPKKKs, including ILK members.

ILK5 has bona fide kinase activity

Both animal and plant ILKs contain conserved regions consistent with a role as serine/threonine or dual serine/threonine and tyrosine protein kinases. Animal ILKs contain abundant substitutions in the conserved residues of the kinase domain and, therefore, their functional role as active kinases has been questioned, with published reports substantiating the view that they are pseudo-kinases (Hannigan et al., 2011). However, relative to animal ILKs, plant ILKs contain fewer substitutions, and the possibility remains the that they possess kinase function. Indeed, Medicago MsILK1 and Arabidopsis AtILK1 have an unusual Mn^{2+} divalent ion dependent kinase activity, which was found to be necessary for root growth and pathogen response (Chinchilla et al., 2008; Brauer et al., 2016). Some of the confusion about ILK kinase function may have to do with the means by which the proteins were purified. For example, in our case with ILK5 as well as in a previous report for ILK1, purification of the proteins from plant tissue was necessary to produce proteins with kinase activity. In the case of ILK1, its kinase activity is essential for mediating plant disease resistance (Brauer et al., 2016).

At present, we have no explanation as to why it is critical to purify these proteins from plant extracts in order to retain kinase activity. It may be that proper protein folding or protein secondary modification in plant tissues may be essential for kinase activation of ILK proteins, including ILK5. In a previous study, according to protein sequence comparison and structural analysis, it was found that ILK4/Raf47, ILK5/Raf27, and ILK6/Raf17 display relatively longer canonical A-loops and/or C-loops in the sub-domains. Alterations in the canonical kinase motifs can lead to atypical reliance on Mn^{2+} as a cofactor in plant ILKs for full kinase activity (Popescu et al., 2017). Regardless, the data clearly indicates that plant ILKs are functional protein kinases and, hence, appear to function as MAPK kinase kinases to activate downstream MAPK cascades.

ILK5 plays a key role in regulation of stomatal aperture and plant stress responses

Our previous publication showed that extracellular ATP elicits P2K1-mediated RBOHD phosphorylation to regulate stomatal closure, enhancing plant innate immunity (Chen et al., 2017). ILK5 is highly expressed in guard cells and highly induced by various stress conditions and was previously demonstrated to play an crucial role in regulation of stomatal aperture (Hayashi et al., 2017). This is also true of P2K1-mediated stomatal closure in that *p2k1* mutants still closed stomates in response to abscisic acid treatment (Chen et al., 2017). The model that emerges from the current study and published results is that purinergic signaling impacts stomatal aperture control, at least in part, via activation of ILK5 and its role in downstream activation of the MAPK cascade.

In addition to playing a role in the plant response to biotic stress, it is also possible that ILK5 is involved in abiotic stress responses. Extracellular ATP accumulates within the apoplast under abiotic stress conditions and, interestingly, P2K1 is also highly induced by various abiotic stress conditions (Supplemental Figure S8F). The expression of several plant *ILK* genes, including *ILK5*, is increased under various abiotic and/or biotic stress conditions (Popescu et al., 2017), similar to P2K1. Considering that purinergic signaling regulates plant growth under various environmental conditions or in response to diverse abiotic and biotic stress conditions, it seems likely that P2K1 and ILK5 work coordinately to mediate the appropriate plant responses to such stresses.

Material and methods

Plant materials and growth conditions

Arabidopsis thaliana ecotype Columbia (Col-0) and T-DNA insertion mutants [WiscDsLox345-348B17 (*ilk5-1*), SALK_099335C (*ilk5-2*), SALK_050039 (*ilk5-3*) and SALK_082479 (*ilk5-4*)] were used in this study. Seeds were sterilized by soaking in 1% bleach solution for 10 min followed by washing five times with sterilized water. Seeds were grown on agar plates for germination. One-half-strength Murashige and Skoog (MS) medium with 1% (w/v) sucrose and 0.5% (w/v) phytagel, 0.05% (w/v) MES, adjusted with KOH to approximately pH 5.7, was used. The plates were then kept in the dark at 4°C for three days for vernalization before being placed in a growth chamber for germination. Seedling plants were transferred to soil and grown to maturity for further experiments. The plants were grown under long-day conditions [16-h days with 150 $\mu E \cdot m^{-2} \cdot s^{-1}$ (E, Einstein; 1 E = 1 mol of photons)] light intensity provided by white LED lamps at 21°C.

Plasmid constructs and transgenic plants

Full-length CDS of *ILK5* (AT4G18950), *ILK6* (AT1G14000), *P2K1* (AT5G60300), *RBOHD* (AT5G47910), *CPK5* (AT4G35310), *MKK3* (AT5G40440), *MKK4* (AT1G51660), *MKK5* (AT3G21220), and *MKK8* (AT3G06230), as well as their kinase domain or C-terminal domain, were amplified by PCR reaction using a set of gene-specific primer pairs (Supplemental Table S1). Each PCR product was sub-cloned into *pDONR-Zeo* (Invitrogen) or *pGEM-T* Easy vectors (Promega) for further experiments. In order to generate YFP constructs, *pAM-PAT-GW-YFP* vector was used. For the BiFC experiment in Arabidopsis protoplasts, *pAM-PAT-GW-cYFP*, and *pAM-PAT-GW-cYFP* gateway vector were C-terminally fused with split-YFP. For the LCI assays in *Nicotiana benthamiana* leaves, the full-length CDS DNAs from the *pDONR-Zeo* vector were cloned into *pCAMBIA1300-GW-nLUC* and *pCAMBIA1300-GW-cLUC* gateway vector. The *ILK5* promoter was cloned as a 2 kb fragment upstream of the *ILK5* translation start codon into the *pDONR-Zeo* vector by BP reaction. *ILK5promoter:GUS* and *GFP* fusions were generated by LR cloning into *pGWB3* (GUS) and *pGWB4* (GFP) gateway vectors, respectively. In order to generate the ILK5 wild-type and ILK5^{S192A} complementation lines, *ILK5* genomic DNA (~4.5 kb), including the 2 kb promoter region, was amplified by PCR reaction using a pair of specific primers and cloned into the *pDONR-Zeo* vector by BP reaction. LR reaction was performed by LR clonase (Invitrogen) with *pGWB13* (HA-tagging) in order to generate the ILK5 wild-type and ILK5^{S192A} complementation lines. GST fused-P2K1 and the kinase dead version of P2K1 (GST-P2K1^{D572N}-CD or GST-P2K1^{D525N}-CD) were described by (Chen et al., 2017) and GST-fused MKK4 and MKK5 were generated by LR reaction into pDEST15 (Invitrogen) gateway vector. In order to generate His-tagged constructs, DNA fragments of *ILK5* and *CPK5* were amplified by PCR reaction and digested with *Eco*RI/*Xho*I and *Bam*HI/*Xho*I, respectively, followed by cloned into the pET21a vector. CPK5^{D221A}, ILK5^{K184A}, ILK5^{S192A}, ILK5^{S192D}, MKK4^{K108R}, MKK5^{K99R} and MKK5^{K99RT215AS221A} were generated by site-directed mutagenesis following the manufacturer's protocol (Invitrogen, Platinum SuperFi DNA polymerase). To obtain transgenic plants, each construct was introduced into *Agrobacterium tumefaciens* strain *GV3101* and Arabidopsis plants were transformed using the 'floral-dip' method (Clough and Bent, 1998).

Kinase Client (KiC) assay

The KiC assay was performed as previously described (Chen et al., 2017; Ahsan et al., 2013). Briefly, a library of more than 2100 peptides developed from identified *in vivo* phosphorylation sites taken from a number of studies was incubated with the purified recombinant GST fused P2K1 kinase domain (GST-P2K1-CD) in the presence of ATP. Two sets of empty vectors (GST and MBP) and two kinase-dead proteins, GST-P2K1^{D572N}-CD and GST-P2K1^{D525N}-CD, were used as negative controls. The peptide reaction mixtures were analyzed using a Finnigan Surveyor Liquid Chromatography system interfaced with a LTQ Orbitrap XL ETD mass spectrometer. For final validation, each spectrum was manually examined and the phosphopeptides were allowed only if the highest pRS site probability, pRS score, Xcorr value, and site-determining fragment ions were observed for the unambiguous location of the phosphorylation site. Phosphopeptides with a pRS score of ≥15 and/or a pRS site probability of ≥50% were accepted.

Subcellular localization of YFP-tagged protein and BiFC assay

YFP or split-YFP protein fusion plasmids (*pAM-PAT-GW-YFP* or *pAM-PAT-YFP-GW* for YFP and *pAM-PAT-GW-nYFP* and *pAM-PAT-GW-cYFP* for split-YFP) were co-transformed by polyethylene glycol (PEG)-mediated transformation into Arabidopsis protoplasts prepared from leaf tissues of three-week-old plants as previously described (Kim et al., 2016). Then, transformed protoplasts were incubated in a 21°C growth chamber for 24 h under dark conditions. The YFP fluorescence was monitored using a Leica DM 5500B compound microscope with Leica DFC290 color digital camera 24 h after transformation. 5 μM FM4-64 (Invitrogen, T3166) was used as a counter stain for the plasma membrane. In addition, 1 μg/mL of 4′-6-diamidino-2-phenylindole (DAPI; Sigma-D9542-10MG) was used as a nuclear marker. For the YFP transgenic plants, YFP constructs driven by the *35S* promoter were transformed into the *A. tumefaciens GV3101*(*pMP90RK*) and Arabidopsis plants were transformed using the 'floral-dip' method (Clough and Bent, 1998). Confocal images were generated using a laser confocal microscope (Leica, TCS SP8 STED) attached to a vertical microscope (Leica MP Color Digital Camera) equipped with various fluorescein filters. The YFP signal was excited at a wavelength of 514 nm under a confocal laser-scanning microscope with an argon ion laser system.

Co-immunoprecipitation assay

GV3101 carrying the indicated constructs in infiltration buffer [10 mM MES (pH 5.7), 10 mM $MgCl_2$, 100 μM 4'-Hydroxy-3',5'-dimethoxyacetophenone] was infiltrated into 4-week-old leaves of *N. benthamiana*. Total protein was purified from co-infiltrated *N. benthamiana* leaf tissues using the protein extraction buffer: 50 mM Tris-HCl (pH 7.5), 150 mM NaCl, 0.2 mM PMSF, 0.5% Triton-X 100, and 1 x protease inhibitor (Thermo Fisher Scientific; A32955) by gentle agitation at 4°C for 2 hours. The solution was centrifuged at 20,000 x g for 15 min at 4°C. The supernatant was decanted in a new e-tube and 30 μL monoclonal anti-HA antibody Agarose beads (Sigma, A2095-1 mL) was added and incubated overnight with end-to-end shaking at 4°C. Subsequently, beads were washed at least 7 times with washing buffer containing 50 mM Tris-HCl (pH 7.5), 150 mM NaCl, and 1 x protease inhibitor. After washing, the resin was eluted with 25 μL 1 x SDS-PAGE loading buffer and the eluent heated in boiling water for 10 min. The proteins were separated by 10% SDS-PAGE and detected by immunoblotting with anti-HA-HRP (Roche, 12013819001; dilution, 1:1000) and anti-Myc (Sigma-Aldrich, SAB4700447; dilution, 1:2000) antibodies.

Split-luciferase complementation imaging (LCI) assay

Each of the constructs containing full-length cDNAs was cloned with split-LUC at their C-termini of the *pCAMBIA1300-GW-nLUC* or *pCAMBIA1300-GW-cLUC* vector and transformed into the *GV3101* by GenePluser^{TM} electro-transformation (BioRad). When the OD_{600} reached 1.0, the cultures were resuspended with infiltration buffer [10 mM MES (pH 5.7), 10 mM $MgCl_2$, 100 μM 4'-Hydroxy-3',5'-dimethoxyacetophenone] and incubated for 2 h. *GV3101* carrying the indicated constructs (OD_{600} = 0.6) was infiltrated into 4-week-old leaves of *N. benthamiana*. The infiltrated leaves were incubated at 28°C for 2 days before LUC activity measurement. 1 mM D-luciferin containing 0.01% silwet-L77 was sprayed onto the *N. benthamiana* leaves and immediately placed in dark conditions for 10 min to quench the fluorescence. The luminescence was monitored and captured using a low light imaging CCD camera (Photek; Photek, Ltd.).

***β*-glucuronidase (GUS) assay**

Whole seedlings or various tissues were immersed in histochemical staining solution containing 1 mM 5-bromo-4-chloro 3-indolyl β-glucuronic acid, 100 mM sodium phosphate (pH 7.0), 0.1 mM EDTA, 0.5 mM ferricyanide, 0.5 mM ferrocyanide and 0.1% Triton-X 100. After incubation in a vacuum for 10 min, the seedlings were incubated at 37°C for 6–12 h depending on staining status. For the wounding treatment, rosette leaves were wounded using hemostat forceps. Chlorophyll was cleared from the plant tissues by immersing them in 70% ethanol then washing with 70% ethanol repeatedly until tissue was clear. Stained tissues were observed by Fisher Stereo-master microscope (FW02-18B-1750) and digital images were obtained using an AmScope digital camera (MU1000).

RT-qPCR analysis

Two-week-old seedling plants were incubated in sterile one-half-strength liquid MS at room temperature overnight. Samples were collected after treatment with 200 μM ATP, 100 nM flg22, *luxCDABE*-tagged *P. syringae* DC3000, drought, heat (37°C), cold (4°C), NaCl (200 mM) or wounding. Total RNA was extracted using Trizol reagent (Invitrogen, 15596018) according to the manufacturer's instructions. The RNA concentration was estimated followed by treatment with Turbo DNA-free DNase (Invitrogen, AM2238). The RNA was used for first-strand cDNA synthesis using reverse transcriptase (Promega, M-MLV Reverse Transcriptase, PRM1705). The real-time qPCR was performed using SYBR^{TM} Green PCR Master mix (Applied Biosystems, Power SYBR® Green PCR Master Mix, 4368702) following the manufacturer's instructions. The gene-specific primers used are listed in Supplemental Table S1. RNA levels were normalized against the expression of *SAND* or *UBIQUITIN* (*UBQ*).

***in vitro* kinase assays**

His-tagged ILK5 (ILK5-His) and CPK5 were fused C-terminally in the *pET21a* vector (Novagen). Plasmids were transformed into Rosetta^{TM} (DE3) competent cells (Novagen). His-tagged proteins were purified by TALON Metal Affinity Resin (Clontech #635502), following the manufacturer's protocol. The GST-tagged cytosolic domain of P2K1 (GST-P2K1-CD) and its kinase dead versions (GST-P2K1^{D572N}-CD and GST-P2K1^{D525N}-CD) were fused N-terminally in the *pGEX-5X-1* vector (GE Healthcare). GST-His-MKK4 and MKK5 protein were fused N-terminally in the pET41a vector (Novagen). Plasmids were

transformed into Rosetta^{TM} (DE3) competent cells expressing YopH tyrosine phosphatase. GST-tagged proteins were purified by Glutathione Resin (GenScript #L00206), following the manufacturer's protocol. N-terminally His-tagged ILK5 (His-ILK5) and GFP (His-GFP) were also purified from *N. benthamiana*. For expression of His-tagged ILK5 and GFP protein in *N. benthamiana* plants, CDS of *ILK5* and GFP were amplified by PCR and digested with *Sma*I/*Xho*I restriction enzyme and ligated into the *pEAQ-HT* vector (Sainsbury et al., 2009). These constructs were introduced into *A. tumefaciens* strain *LBA4404* and infiltrated into leaves from 4-6 weeks old *N. benthamiana*. In order to extract the His-ILK5 and His-GFP protein from *N. benthamiana* plants, we followed the previous protocols (Sainsbury et al., 2009; Souza, 2015). *in vitro* kinase assay was performed as previously described with minor modifications (Lu et al., 2010, 1). Briefly, 2 μg of purified GST or GST-tagged protein kinases were incubated with 2 μg His-tagged ILK5 protein as a substrate in a 25 μL reaction buffer containing 20 mM Tris-HCl (pH 7.4), 5 mM $MgCl_2$ or $MnCl_2$, 100 mM NaCl, 2 mM ATP, with or without 0.2 μL radioactive [γ-^{32}P] ATP for 1 h at 30°C. Kinase activity over time was measured at 0 h and then at 1-h intervals for 3h. The two reactions with or without radioactive [γ-^{32}P] ATP reactions were stopped by adding 5 μL of 5 × SDS loading buffer and incubating in the thermomixer (Eppendorf, 22331Hamburg) at 100°C for 5 min. Each reaction was separated by electrophoresis in 12% SDS-PAGE gels, and the gel containing radioactive [γ-^{32}P] ATP was auto-radiographed using a Typhoon FLA 9000 Phospho-imager (GE Healthcare) for 12 h. Either reaction mixture with or without radioactive [γ-^{32}P] ATP were stained with Coomassie Brilliant Blue (CBB) and used as a loading control.

MAPK phosphorylation and immunoblot assay

Total protein was extracted from 10-day-old transgenic Arabidopsis plants or leaf discs from 4-week-old plants, at the indicated time points treated with 250 μM ATP or ATPγS by homogenization. Total protein was extracted with extraction buffer containing 50 mM Tris-HCl (pH 7.5), 150 mM NaCl, 10 mM $MgCl_2$, 1 mM EDTA, 1 mM DTT, 0.2 mM Phenylmethylsulfonyl fluoride (PMSF; Sigma, 93482), 10% glycerol, 0.5% Triton-X 100, and 1 x protease inhibitor (Sigma Aldrich, PIA32955) at 4°C with gentle agitation for 2 h to extract total protein from the plant tissues. The samples were centrifuged at 20,000 x g for 15 min at 4°C. Supernatant was transferred to e-tube and centrifuged again at 20,000 x g for 10 min at 4°C, to pellet any carryover leaf debris. The extracted total proteins were mixed with 5 x Laemmli loading buffer

containing 10% SDS, 50% glycerol, 0.01% bromophenol blue, 10% β-mercaptoethanol, 0.3 M Tris-HCl pH 6.8, and heated in boiling water for 5 min. The total extracted proteins were separated by 10 or 12% SDS-PAGE gel and detected by immunoblotting with anti-phospho-p44/p42 MAPK antibody (Cell signaling, 4370L; dilution, 1:2000), anti-HA-HRP antibody (Roche, 12013819001; dilution 1:2000), anti-GFP antibodies (Invitrogen, A11122; dilution 1:4000 and Santa Cruz, sc-8334; dilution 1:2000), anti-luciferase (nLUC) antibody (Sigma, L0159; dilution 1:5000), anti-cLUC antibody (Sigma, L2164; dilution 1:4000) anti-MPK3 (dilution 1:2000) and MPK6 (dilution 1:4000) antibodies (Besteiro and Ulm, 2013; Jiang et al., 2017).

***In vivo* kinase assay**

100 μg of *pUGW-CPK5-HA* or *pUGW-ILK5-HA* constructs were introduced by PEG-mediated transformation into Arabidopsis protoplasts prepared from leaf tissues of four-week-old plants described above, then incubated in a 21°C growth chamber for 48 h under dark conditions with 2 mL W5 solution (2 mM MES pH 5.7, 154 mM NaCl, 125 mM $CaCl_2$, and 5 mM KCl). 250 μM ATP or ATPγS was added and incubated for 1 hour at 21°C. All intact protoplasts were then subsequently harvested by centrifugation at 50 × g for 4 min at room temperature. All supernatant was removed and 250 μL of total protein extraction buffer [50 mM Tris-HCl (pH 7.5), 150 mM NaCl, 0.2 mM PMSF, 0.5% Triton-X 100, and 1 x protease inhibitor was added and incubated 4°C for 2 h. Immunoprecipitations were performed as described above. The proteins were separated by SDS-PAGE and immunoblotting was carried out using anti-HA-HRP (Roche, 12013819001; dilution 1:2000) and anti-phospho-Ser/Thr (BD Transduction laboratories, 612548, dilution 1:6000) antibodies.

GST pull-down assay

Recombinant proteins GST and GST-MKK5 fused N-terminally in the *pGEX-5X-1* vector were expressed in *E. coli* and affinity purified using Glutathione Resin (GenScript, L00206). His-ILK5 and His-GFP proteins were expressed using *LBA4404* Agrobacterium His tagged proteins were purified using TALON® Metal Affinity Resin (Clontech, 635502). For GST pull-down, 5 μg of GST and His recombinant proteins were incubated with protein binding buffer (50 mM Tris-HCl pH 7.5, 100 mM NaCl, and 0.5% Triton-X100), then subjected to end-to-end shaking for 4 h at 4°C. After taking 20 μL as an input, 50 μL

Glutathione Resin beads were added and incubated for 2 h, and then washed seven times with protein binding buffer. The protein was eluted by 50 μL 1× SDS-PAGE loading buffer and heated at 100°C for 10 min. The proteins were separated using 10% SDS-PAGE gels and detected by immunoblotting using anti-His antibody (Sigma, SAB1305538; dilution, 1:4000) and anti-GST-HRP antibody (GenScript, A01380-40; dilution, 1:2000).

Bacterial growth assays

Two- or three-week-old plants were flood inoculated with a suspension of *luxCDABE*-tagged *P. syringae* DC3000 cells (OD_{600} = 0.002 approximately 5×10^6 CFU mL^{-1}) containing 10 mM MES pH 5.7, 10 mM $MgCl_2$ and 0.025% (v/v) Silwet L-77 with or without the addition of 250 μM ATP in the bacterial suspensions. The bacterial suspension was incubated for 3 min and immediately removed by decantation and the plates containing inoculated plants were incubated in the plant chamber under long-day conditions (16-h days with 150 $\mu E \cdot m^{-2} \cdot s^{-1}$) at 21°C. Three days post inoculation, plants were washed with ddH_2O for 5 min. The plants without roots were ground in 10 mM $MgCl_2$, diluted serially, and plated on LB agar with 25 mg/L rifampicin. Colonies (CFU) were counted after incubation at 28°C for 2 days.

Stomatal closure experiment

Four-week-old plants were placed under light for 2 h in order to ensure that the starting plants had fully open stomata. Leaf peels were obtained from the abaxial side by tweezers and incubated in a stomata buffer containing 10 mM MES (pH 6.15), 10 mM KCl, and 10 μM $CaCl_2$. These peels were treated with 2 mM ATP, 5 μM ABA (Sigma, A1049) or mock solution for 1 h and then images captured using a light microscope (Nikon, Alphaphot2). The stomatal aperture was measured using ImageJ software (Version 1.51a).

Accession numbers

Sequence data for the genes described in this study can be found at The Arabidopsis Information Resource (TAIR) under the following accession numbers: P2K1 (At5g60300), ILK5 (At4g18950), CPK5 (At4g35310), MKK3 (At5g40440), MKK4 (At1g51660), MKK5 (At3g21220), MKK8 (At3g06230),

ILK1 (At2g43850), ILK6 (At1g14000), RBOHD (At5g47910), WRKY40 (At1g80840), CPK28 (At5g66210), and SID2 (At1g74710).

Data availability

The mass spectrometry proteomics data are available at the ProteomeXchange Consortium via the PRIDE partner repository with the data set identifier PXD006678. The authors declare that all other data supporting the findings of this study are available within the manuscript and its supplementary files or are available from the corresponding author on request.

Acknowledgments

We thank to Dr. Jian-Min Zhou (Chinese Academy of Sciences) for providing *mapkkk3-2 mapkkk5-2* and *mapkkk3-3 mapkkk5-2* mutants, and Dr. Scott Peck (University of Missouri) for providing anti-MPK3 and -MPK6 antibodies and pep1 elicitor. We also thank current and former members in Gary Stacey laboratory, especially Samantha Yanders, Sung-Hwan Cho and Jared Ellingsen for aid in writing this manuscript.

Funding

This work was supported by the National Institute of General Medical Sciences of the National Institutes of Health (grant no. R01GM121445), the Next-Generation BioGreen 21 Program Systems and Synthetic Agrobiotech Center, Rural Development Administration, Republic of Korea (grant no. PJ01325403), through the 3rd call of the ERA-NET for Coordinating Action in Plant Sciences, with funding from the US National Science Foundation (NSF, grant no. 1826803) and funding from the NSF Plant Genome Research Program (grant no. 2048410).

Author contributions

D.K. designed and performed the experiments; N.A. and J.J.T. performed and supervised the kinase client assay for screening of P2K1 targets. D.C. performed Co-IP analysis. G.L.J performed mass-spec analysis of His-ILK5 protein from *N. benthamiana*. G.S. supervised the study and edited the manuscript. All authors discussed the results and commented on the manuscript.

Conflict of interest statement. The authors declare no conflict of interest.

References

Ahsan, N., Huang, Y., Tovar-Mendez, A., Swatek, K.N., Zhang, J., Miernyk, J.A., Xu, D., and Thelen, J.J. (2013). A versatile mass spectrometry-based method to both identify kinase client-relationships and characterize signaling network topology. J Proteome Res **12**: 937–948.

Asai, T., Tena, G., Plotnikova, J., Willmann, M.R., Chiu, W.-L., Gomez-Gomez, L., Boller, T., Ausubel, F.M., and Sheen, J. (2002). MAP kinase signalling cascade in Arabidopsis innate immunity. Nature **415**: 977–983.

Bagchi, S., Liao, Z., Gonzalez, F.A., Chorna, N.E., Seye, C.I., Weisman, G.A., and Erb, L. (2005). The P2Y2 Nucleotide Receptor Interacts with αv Integrins to Activate Go and Induce Cell Migration. J. Biol. Chem. **280**: 39050–39057.

Balagué, C., Gouget, A., Bouchez, O., Souriac, C., Haget, N., Boutet-Mercey, S., Govers, F., Roby, D., and Canut, H. (2017). The Arabidopsis thaliana lectin receptor kinase LecRK-I.9 is required for full resistance to Pseudomonas syringae and affects jasmonate signalling. Mol Plant Pathol **18**: 937–948.

Besteiro, M.A.G. and Ulm, R. (2013). Phosphorylation and Stabilization of Arabidopsis MAP Kinase Phosphatase 1 in Response to UV-B Stress *. Journal of Biological Chemistry **288**: 480–486.

Bi, G., Zhou, Z., Wang, W., Li, L., Rao, S., Wu, Y., Zhang, X., Menke, F.L.H., Chen, S., and Zhou, J.-M. (2018). Receptor-Like Cytoplasmic Kinases Directly Link Diverse Pattern Recognition Receptors to the Activation of Mitogen-Activated Protein Kinase Cascades in Arabidopsis. The Plant Cell **30**: 1543–1561.

Bouwmeester, K., Han, M., Blanco-Portales, R., Song, W., Weide, R., Guo, L.-Y., van der Vossen, E.A.G., and Govers, F. (2014). The Arabidopsis lectin receptor kinase LecRK-I.9 enhances resistance to Phytophthora infestans in Solanaceous plants. Plant Biotechnol J **12**: 10–16.

Bouwmeester, K., de Sain, M., Weide, R., Gouget, A., Klamer, S., Canut, H., and Govers, F. (2011). The lectin receptor kinase LecRK-I.9 is a novel Phytophthora resistance component and a potential host target for a RXLR effector. PLoS Pathog **7**: e1001327.

Brauer, E.K., Ahsan, N., Dale, R., Kato, N., Coluccio, A.E., Piñeros, M.A., Kochian, L.V., Thelen, J.J., and Popescu, S.C. (2016). The Raf-like Kinase ILK1 and the High Affinity K+ Transporter HAK5 Are Required for Innate Immunity and Abiotic Stress Response1[OPEN]. Plant Physiol **171**: 1470–1484.

Bye, A.P., Gibbins, J.M., and Mahaut-Smith, M.P. (2020). Ca2+ waves coordinate purinergic receptor–evoked integrin activation and polarization. Sci. Signal. **13**.

Cao, Y., Tanaka, K., Nguyen, C.T., and Stacey, G. (2014). Extracellular ATP is a central signaling molecule in plant stress responses. Curr Opin Plant Biol **20**: 82–87.

Cekic, C. and Linden, J. (2016). Purinergic regulation of the immune system. Nat Rev Immunol **16**: 177–192.

Chen, D., Cao, Y., Li, H., Kim, D., Ahsan, N., Thelen, J., and Stacey, G. (2017). Extracellular ATP elicits DORN1-mediated RBOHD phosphorylation to regulate stomatal aperture. Nat Commun **8**: 2265.

Chen, D., Hao, F., Mu, H., Ahsan, N., Thelen, J.J., and Stacey, G. (2021). S-acylation of P2K1 mediates extracellular ATP-induced immune signaling in Arabidopsis. Nat Commun **12**: 2750.

Chinchilla, D., Frugier, F., Raices, M., Merchan, F., Giammaria, V., Gargantini, P., Gonzalez-Rizzo, S., Crespi, M., and Ulloa, R. (2008). A mutant ankyrin protein kinase from Medicago sativa affects Arabidopsis adventitious roots. Functional Plant Biol. **35**: 92.

Chinchilla, D., Merchan, F., Megias, M., Kondorosi, A., Sousa, C., and Crespi, M. (2003). Ankyrin protein kinases: a novel type of plant kinase gene whose expression is induced by osmotic stress in alfalfa. Plant Mol Biol **51**: 555–566.

Chivasa, S., Ndimba, B.K., Simon, W.J., Lindsey, K., and Slabas, A.R. (2005). Extracellular ATP functions as an endogenous external metabolite regulating plant cell viability. Plant Cell **17**: 3019–3034.

Cho, S.-H., Tóth, K., Kim, D., Vo, P.H., Lin, C.-H., Handakumbura, P.P., Ubach, A.R., Evans, S., Paša-Tolić, L., and Stacey, G. (2022). Activation of the plant mevalonate pathway by extracellular ATP. Nat Commun **13**: 450.

Choi, J. (2013). Identification of an Extracellular Adenosine 5'-triphosphate Receptor in Arabidopsis Thaliana.

Choi, J., Tanaka, K., Cao, Y., Qi, Y., Qiu, J., Liang, Y., Lee, S.Y., and Stacey, G. (2014a). Identification of a Plant Receptor for Extracellular ATP. Science **343**: 290–294.

Choi, J., Tanaka, K., Liang, Y., Cao, Y., Lee, S.Y., and Stacey, G. (2014b). Extracellular ATP, a danger signal, is recognized by DORN1 in Arabidopsis. Biochem J **463**: 429–437.

Clark, G., Fraley, D., Steinebrunner, I., Cervantes, A., Onyirimba, J., Liu, A., Torres, J., Tang, W., Kim, J., and Roux, S.J. (2011). Extracellular Nucleotides and Apyrases Regulate Stomatal Aperture in Arabidopsis1[W][OA]. Plant Physiol **156**: 1740–1753.

Clark, K.L., Larsen, P.B., Wang, X., and Chang, C. (1998). Association of the Arabidopsis CTR1 Raf-like kinase with the ETR1 and ERS ethylene receptors. Proc Natl Acad Sci U S A **95**: 5401–5406.

Clough, S.J. and Bent, A.F. (1998). Floral dip: a simplified method for Agrobacterium-mediated transformation of Arabidopsis thaliana. Plant J **16**: 735–743.

CristinaRodriguez, M., Petersen, M., and Mundy, J. (2010). Mitogen-Activated Protein Kinase Signaling in Plants. Annu Rev Plant Biol **61**: 621–649.

Dagnino, L. (2011). Integrin-linked kinase: a Scaffold protein unique among its ilk. J Cell Commun Signal **5**: 81–83.

Deng, S. et al. (2015). Populus euphratica APYRASE2 Enhances Cold Tolerance by Modulating Vesicular Trafficking and Extracellular ATP in Arabidopsis Plants. Plant Physiol **169**: 530–548.

Desgrosellier, J.S. and Cheresh, D.A. (2010). Integrins in cancer: biological implications and therapeutic opportunities. Nat Rev Cancer **10**: 9–22.

Duong, H.N., Cho, S.-H., Wang, L., Pham, A.Q., Davies, J.M., and Stacey, G. (2021). Cyclic Nucleotide Gated Ion Channel 6 is involved in extracellular ATP signaling and plant immunity. Plant J.

Faria, R., Ferreira, L., Bezerra, R., Frutuoso, V., and Alves, L. (2012). Action of natural products on p2 receptors: a reinvented era for drug discovery. Molecules **17**: 13009–13025.

Feng, H., Guan, D., Bai, J., Sun, K., and Jia, L. (2015). Extracellular ATP: a potential regulator of plant cell death. Mol Plant Pathol **16**: 633–639.

Ferrari, D., McNamee, E.N., Idzko, M., Gambari, R., and Eltzschig, H.K. (2016). Purinergic Signaling During Immune Cell Trafficking. Trends Immunol **37**: 399–411.

Frye, C.A. and Innes, R.W. (1998). An Arabidopsis mutant with enhanced resistance to powdery mildew. Plant Cell **10**: 947–956.

Frye, C.A., Tang, D., and Innes, R.W. (2001). Negative regulation of defense responses in plants by a conserved MAPKK kinase. Proc Natl Acad Sci U S A **98**: 373–378.

Hannigan, G.E., Leung-Hagesteijn, C., Fitz-Gibbon, L., Coppolino, M.G., Radeva, G., Filmus, J., Bell, J.C., and Dedhar, S. (1996). Regulation of cell adhesion and anchorage-dependent growth by a new β1-integrin-linked protein kinase. Nature **379**: 91–96.

Hannigan, G.E., McDonald, P.C., Walsh, M.P., and Dedhar, S. (2011). Integrin-linked kinase: Not so 'pseudo' after all. Oncogene **30**: 4375–4385.

Hayashi, M., Inoue, S.-I., Ueno, Y., and Kinoshita, T. (2017). A Raf-like protein kinase BHP mediates blue light-dependent stomatal opening. Sci Rep **7**: 45586.

Huang, Y., Houston, N.L., Tovar-Mendez, A., Stevenson, S.E., Miernyk, J.A., Randall, D.D., and Thelen, J.J. (2010). A quantitative mass spectrometry-based approach for identifying protein kinase clients and quantifying kinase activity. Anal Biochem **402**: 69–76.

Hynes, R.O. (2002). Integrins: Bidirectional, Allosteric Signaling Machines. Cell **110**: 673–687.

Jiang, L., Anderson, J.C., Besteiro, M.A.G., and Peck, S.C. (2017). Phosphorylation of Arabidopsis MAP Kinase Phosphatase 1 (MKP1) Is Required for PAMP Responses and Resistance against Bacteria1[OPEN]. Plant Physiol **175**: 1839–1852.

Kieber, J.J., Rothenberg, M., Roman, G., Feldmann, K.A., and Ecker, J.R. (1993). CTR1, a negative regulator of the ethylene response pathway in Arabidopsis, encodes a member of the raf family of protein kinases. Cell **72**: 427–441.

Kim, C., Ye, F., and Ginsberg, M.H. (2011). Regulation of Integrin Activation. Annu Rev Cell Dev Biol **27**: 321–345.

Kim, D.W., Jeon, S.J., Hwang, S.M., Hong, J.C., and Bahk, J.D. (2016). The C3H-type zinc finger protein GDS1/C3H42 is a nuclear-speckle-localized protein that is essential for normal growth and development in Arabidopsis. Plant Sci **250**: 141–153.

Kim, S.-Y., Sivaguru, M., and Stacey, G. (2006). Extracellular ATP in plants. Visualization, localization, and analysis of physiological significance in growth and signaling. Plant Physiol **142**: 984–992.

Knepper, C., Savory, E.A., and Day, B. (2011). Arabidopsis NDR1 Is an Integrin-Like Protein with a Role in Fluid Loss and Plasma Membrane-Cell Wall Adhesion. Plant Physiol **156**: 286–300.

Le, T.-T.T., Berg, N.K., Harting, M.T., Li, X., Eltzschig, H.K., and Yuan, X. (2019). Purinergic Signaling in Pulmonary Inflammation. Front. Immunol. **10**.

Lew, R.R. and Dearnaley, J.D.W. (2000). Extracellular nucleotide effects on the electrical properties of growing Arabidopsis thaliana root hairs. Plant Science **153**: 1–6.

Liang, X. and Zhou, J.-M. (2018). Receptor-Like Cytoplasmic Kinases: Central Players in Plant Receptor Kinase–Mediated Signaling. Annu Rev Plant Biol **69**: 267–299.

Lu, D., Wu, S., Gao, X., Zhang, Y., Shan, L., and He, P. (2010). A receptor-like cytoplasmic kinase, BIK1, associates with a flagellin receptor complex to initiate plant innate immunity. Proc Natl Acad Sci U S A **107**: 496–501.

MAPK Group (2002). Mitogen-activated protein kinase cascades in plants: a new nomenclature. Trends Plant Sci **7**: 301–308.

Markou, T., Vassort, G., and Lazou, A. (2003). Regulation of MAPK pathways in response to purinergic stimulation of adult rat cardiac myocytes. Mol Cell Biochem **242**: 163–171.

Matzinger, P. (2007). Friendly and dangerous signals: is the tissue in control? Nat Immunol **8**: 11–13.

Meder, B. et al. (2011). PINCH Proteins Regulate Cardiac Contractility by Modulating Integrin-Linked Kinase-Protein Kinase B Signaling▿. Mol Cell Biol **31**: 3424–3435.

Myers, R.J., Fichman, Y., Stacey, G., and Mittler, R. (2022). Extracellular ATP plays an important role in systemic wound response activation.: 2022.01.06.475278.

Neary, J.T., Kang, Y., Bu, Y., Yu, E., Akong, K., and Peters, C.M. (1999). Mitogenic Signaling by ATP/P2Y Purinergic Receptors in Astrocytes: Involvement of a Calcium-Independent Protein Kinase C, Extracellular Signal-Regulated Protein Kinase Pathway Distinct from the Phosphatidylinositol-Specific Phospholipase C/Calcium Pathway. J Neurosci **19**: 4211–4220.

Nemoto, K., Seto, T., Takahashi, H., Nozawa, A., Seki, M., Shinozaki, K., Endo, Y., and Sawasaki, T. (2011). Autophosphorylation profiling of Arabidopsis protein kinases using the cell-free system. Phytochemistry **72**: 1136–1144.

Pham, A.Q., Cho, S.-H., Nguyen, C.T., and Stacey, G. (2020). Arabidopsis Lectin Receptor Kinase P2K2 Is a Second Plant Receptor for Extracellular ATP and Contributes to Innate Immunity. Plant Physiol **183**: 1364–1375.

Popescu, S.C., Brauer, E.K., Dimlioglu, G., and Popescu, G.V. (2017). Insights into the Structure, Function, and Ion-Mediated Signaling Pathways Transduced by Plant Integrin-Linked Kinases. Front Plant Sci **8**.

Popescu, S.C., Popescu, G.V., Bachan, S., Zhang, Z., Gerstein, M., Snyder, M., and Dinesh-Kumar, S.P. (2009). MAPK target networks in Arabidopsis thaliana revealed using functional protein microarrays. Genes Dev **23**: 80–92.

Sainsbury, F., Thuenemann, E.C., and Lomonossoff, G.P. (2009). pEAQ: versatile expression vectors for easy and quick transient expression of heterologous proteins in plants. Plant Biotechnol J **7**: 682–693.

Salmaso, V. and Jacobson, K.A. (2020). Purinergic Signaling: Impact of GPCR Structures on Rational Drug Design. ChemMedChem **15**: 1958–1973.

Schultze-Mosgau, A., Katzur, A.C., Arora, K.K., Stojilkovic, S.S., Diedrich, K., and Ortmann, O. (2000). Characterization of calcium-mobilizing, purinergic P2Y2 receptors in human ovarian cancer cells. Mol Hum Reprod **6**: 435–442.

Song, C.J., Steinebrunner, I., Wang, X., Stout, S.C., and Roux, S.J. (2006). Extracellular ATP induces the accumulation of superoxide via NADPH oxidases in Arabidopsis. Plant Physiol **140**: 1222–1232.

Souza, A. de (2015). Expression and Partial Purification of His-tagged Proteins in a Plant System. Bio-protocol **5**: e1572–e1572.

Tang, W., Brady, S.R., Sun, Y., Muday, G.K., and Roux, S.J. (2003). Extracellular ATP inhibits root gravitropism at concentrations that inhibit polar auxin transport. Plant Physiol **131**: 147–154.

Thevananther, S., Sun, H., Li, D., Arjunan, V., Awad, S.S., Wyllie, S., Zimmerman, T.L., Goss, J.A., and Karpen, S.J. (2004). Extracellular ATP activates c-jun N-terminal kinase signaling and cell cycle progression in hepatocytes. Hepatology **39**: 393–402.

Thomas, C., Rajagopal, A., Windsor, B., Dudler, R., Lloyd, A., and Roux, S.J. (2000). A Role for Ectophosphatase in Xenobiotic Resistance. Plant Cell **12**: 519–534.

Thulasi Devendrakumar, K., Li, X., and Zhang, Y. (2018). MAP kinase signalling: interplays between plant PAMP- and effector-triggered immunity. Cell Mol Life Sci **75**: 2981–2989.

Tripathi, D., Zhang, T., Koo, A.J., Stacey, G., and Tanaka, K. (2018). Extracellular ATP Acts on Jasmonate Signaling to Reinforce Plant Defense1[OPEN]. Plant Physiol **176**: 511–523.

Tu, Y., Huang, Y., Zhang, Y., Hua, Y., and Wu, C. (2001). A New Focal Adhesion Protein That Interacts with Integrin-Linked Kinase and Regulates Cell Adhesion and Spreading. J Cell Biol **153**: 585–598.

Wang, L. et al. (2022). Arabidopsis thaliana CYCLIC NUCLEOTIDE-GATED CHANNEL2 mediates extracellular ATP signal transduction in root epidermis. New Phytol.

Wang, Y., Nsibo, D.L., Juhar, H.M., Govers, F., and Bouwmeester, K. (2016). Ectopic expression of Arabidopsis L-type lectin receptor kinase genes LecRK-I.9 and LecRK-IX.1 in Nicotiana benthamiana confers Phytophthora resistance. Plant Cell Rep **35**: 845–855.

Weerasinghe, R.R., Swanson, S.J., Okada, S.F., Garrett, M.B., Kim, S.-Y., Stacey, G., Boucher, R.C., Gilroy, S., and Jones, A.M. (2009). Touch induces ATP release in Arabidopsis roots that is modulated by the heterotrimeric G-protein complex. FEBS Lett **583**: 2521–2526.

Wu, C. and Dedhar, S. (2001). Integrin-linked kinase (ILK) and its interactors. J Cell Biol **155**: 505–510.

Yamada, K. et al. (2016). The Arabidopsis CERK1-associated kinase PBL27 connects chitin perception to MAPK activation. EMBO J **35**: 2468–2483.

Yoo, S.-D., Cho, Y.-H., Tena, G., Xiong, Y., and Sheen, J. (2008). Dual control of nuclear EIN3 by bifurcate MAPK cascades in C2H4 signalling. Nature **451**: 789–795.

Zhu, R., Dong, X., Hao, W., Gao, W., Zhang, W., Xia, S., Liu, T., and Shang, Z. (2017). Heterotrimeric G Protein-Regulated Ca2+ Influx and PIN2 Asymmetric Distribution Are Involved in Arabidopsis thaliana Roots' Avoidance Response to Extracellular ATP. Front Plant Sci **8**: 1522.

.

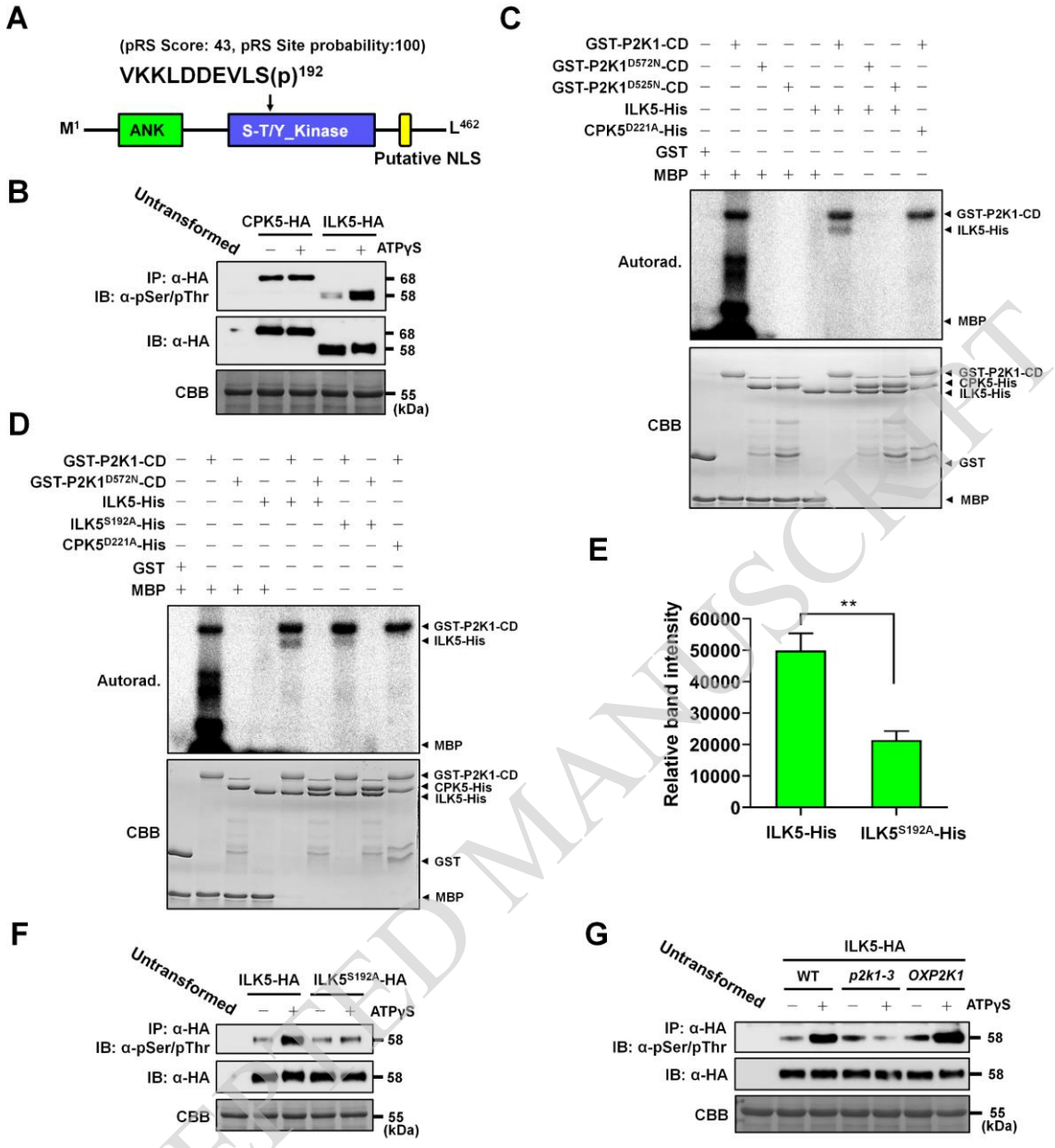

Figure 1. P2K1 directly phosphorylates ILK5. (A) Schematic diagram of ILK5 showing the ankyrin repeat (ANK) and serine-threonine or tyrosine kinase (S-T/Y_kinase) domains. Identified phosphopeptide VKKLDDEVLS(p)^{192} is located in the kinase domain. **(B)** ILK5 protein is phosphorylated by ATPγS treatment *in vivo*. ILK5-HA protein is expressed in Arabidopsis protoplasts upon addition of 250 *μ*M ATPγS and subsequently immunoprecipitated (IP) by anti-HA antibody beads and immunoblotting (IB) is carried out with an anti-phospho-Ser/Thr antibody. CPK5-HA used as a negative control. **(C)** GST-P2K1-CD directly phosphorylates ILK5-His but not CPK5^{D221A}-HA *in vitro*. Bacterial recombinant ILK5-His protein was incubated with GST-P2K1 cytosolic domain (GST-P2K1-CD) or two P2K1 kinase dead versions (GST-P2K1^{D572N}-CD and GST-P2K1^{D525N}-CD), or GST in an *in vitro* kinase assay. **(D)** Mutation of ILK5 on Ser192 residue leads to reduced phosphorylation by P2K1 *in vitro*. Purified GST or GST-P2K1-CD recombinant protein was incubated with ILK5-His or ILK5^{S192A}-His, followed by an *in vitro* kinase assay. In panel C and D, auto- and trans-phosphorylation were detected by incorporation of γ-[^{32}P]-ATP. MBP and CPK5^{D221A}-His were used as a universal substrate and a negative control, respectively. **(E)** Quantification of phosphorylated ILK5 and ILK5^{S192A} protein. The intensity of the phosphorylation signals of ILK5 and ILK5^{S192A} by P2K1-CD (shown in Supplemental Figure 1B) were measured and analyzed using the Image J and GraphPad Prism 8 program. Data shown as mean ± SEM, n = 4, $^{**}p<0.01$, *p*-value indicates significance relative to band intensity of ILK5^{WT}-His and was determined by unpaired two-tailed Student's *t* test. **(F)** Mutation of ILK5 at Ser192 residue results in reduced phosphorylation under ATPγS treatment *in vivo*. Either wild-type or S192A of ILK5-HA (ILK5^{S192A}) protein is expressed in protoplasts upon addition of 250 *μ*M ATPγS and subsequently immunoprecipitated with an anti-HA antibody and immunoblotting is carried out with an anti-phospho-Ser/Thr antibody. **(G)** ILK5 phosphorylation is dependent on P2K1 protein. ILK5-HA protein was expressed in wild-type, *p2k1-3* and *OXP2K1* protoplasts with/without 250 *μ*M ATPγS treatment then subjected to IP and IB by anti-HA and anti-phospho-Ser/Thr antibodies. In panel **(B)**-**(G)**, protein loading was visualized by Coomassie brilliant blue (CBB) staining. Above experiments were repeated at least two times with similar results.

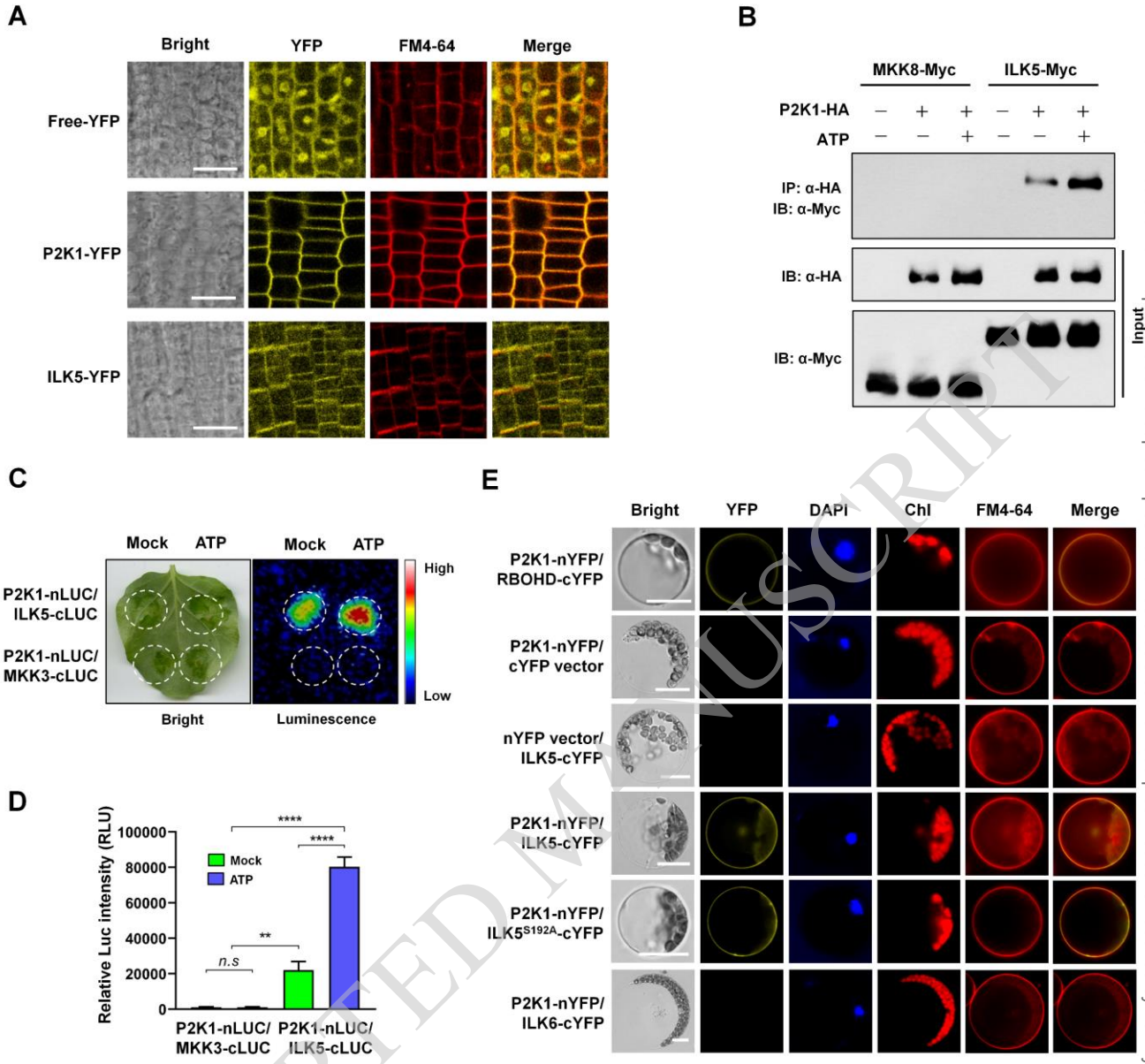

Figure 2. ILK5 interacts with the P2K1 receptor. (A) Subcellular localization of ILK5 in plants expressing a *35S:ILK5-YFP* construct. Fluorescent confocal images displaying the subcellular distribution of ILK5-YFP protein were detected from primary root tissue of seven-day-old seedlings. Plasma membrane was counter-stained by incubation for 1 min in a FM4-64 solution (5 *μ*M). P2K1-YFP and free-YFP were used as controls. FM4-64 was used as a plasma membrane marker. Merge indicates overlapped YFP and FM4-64 images. Scale bars = 50 *μ*m. **(B)** Co-immunoprecipitation of P2K1 and ILK5 proteins. The indicated constructs were co-infiltrated and transiently expressed in *N. benthamiana* leaves after addition of 200 *μ*M ATP (+) for 30 min or MES buffer (pH 5.7) as a mock treatment (−). Total protein was used for Co-IP. Anti-HA and anti-Myc antibodies were used. MKK8-Myc was used as a negative control. **(C)** Split-luciferase experiment showing interaction of P2K1-ILK5 protein with/without ATP treatment. Split-luciferase imaging assay was performed after addition of 200 *μ*M ATP or MES buffer (pH 5.7) as a mock treatment in *N. benthamiana* leaves co-infiltrated with *GV3101* expressing P2K1-nLUC and ILK5-cLUC. 1 mM D-luciferin containing 0.01% silwet L77 was sprayed onto the *N. benthamiana* leaves and immediately placed in dark conditions for 10 min to quench the fluorescence. The luminescence was monitored and captured using a low light imaging CCD camera (Photek; Photek, Ltd.). Dotted circles indicate the infiltrated area in *N. benthamiana* leaves. MKK3-cLUC protein was used as a negative control. **(D)** Quantification of P2K1-ILK5 interaction signal intensities with/without ATP treatment. P2K1-ILK5 interaction was monitored, images were captured, and the luciferase signal intensities were quantified using the C-vision/Im32 and analyzed using the GraphPad Prism 8 program. Data shown as mean ± SEM, n = 4 (biological replicates), ****p<0.0001, ***p<0.001, **p<0.01, *p<0.05, p-value indicates significance relative to MKK3-cLUC and was determined by unpaired two-tailed Student's t test. **(E)** Biomolecular fluorescence complementation (BiFC) assay in Arabidopsis protoplasts. The indicated constructs were transiently transformed into Arabidopsis protoplasts and then incubated under dark conditions for 24 h. The YFP fluorescence was monitored using a Leica DM 5500B Compound Microscope with Leica DFC290 Color Digital Camera. DAPI and FM4-64 were used as a nuclear marker and plasma membrane marker, respectively. Chl represents chlorophyll auto-fluorescence signal. Merge indicates overlapped image of YFP and FM4-64. RBOHD-cYFP and ILK6-cYFP were used as positive and negative control, respectively. Scale bars = 10 *μ*m. All above experiments were repeated three times (biological replicates) with similar results.

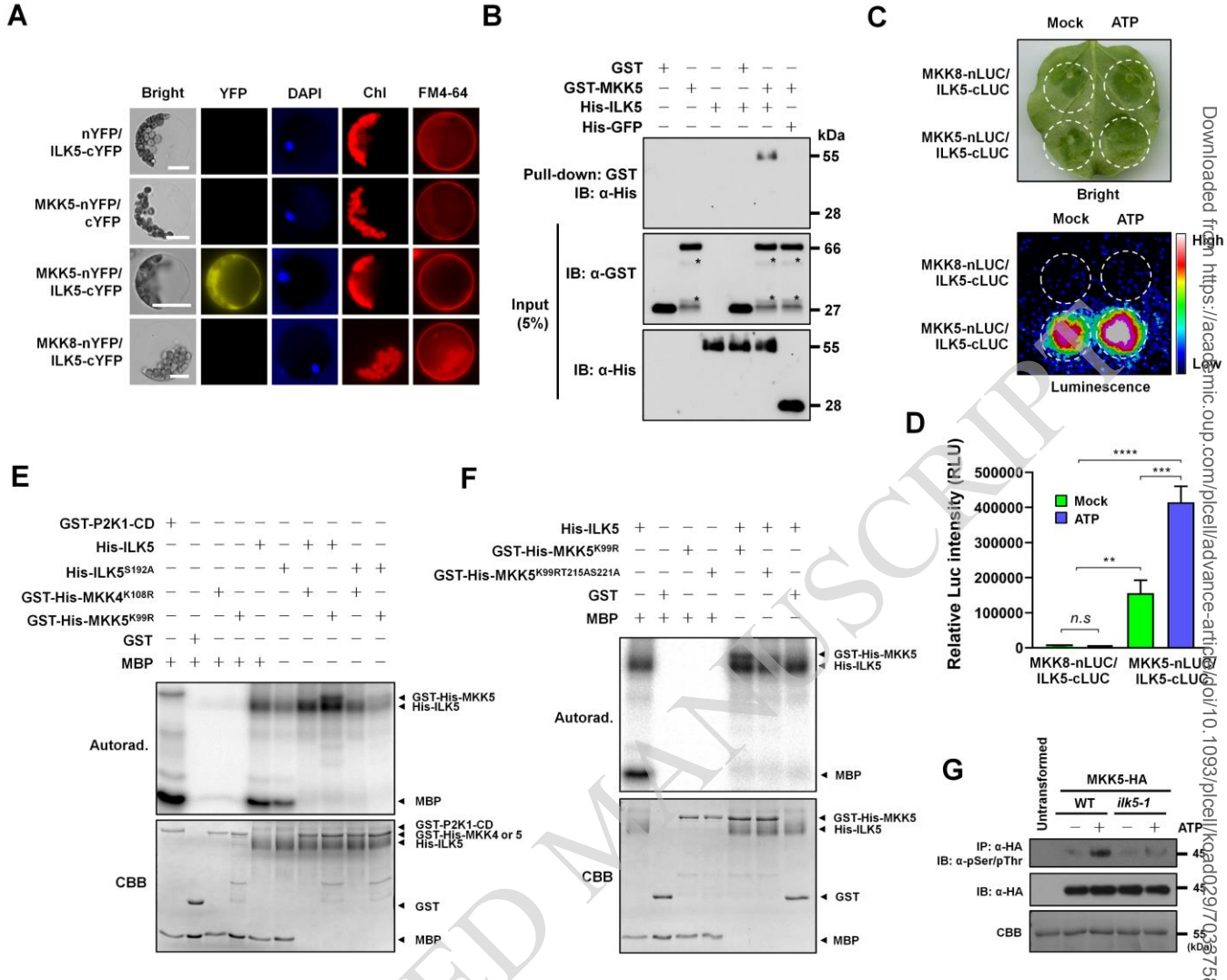

Figure 3. ILK5 interacts with and phosphorylates MKK5 protein. (A) BiFC assay in Arabidopsis protoplasts demonstrating ILK5 interaction with MKK5. The indicated constructs were transiently expressed in Arabidopsis protoplasts and transformed protoplasts were incubated under dark conditions for 24 h before observation YFP signal. The YFP fluorescence was monitored using a Leica DM 5500B Compound Microscope with Leica DFC290 Color Digital Camera. DAPI was used as a nuclear marker. MKK8-nYFP was used as a negative control. Scale bars = 10 *μ*m. **(B)** ILK5 protein directly interacts with MKK5 protein *in vitro*. Purified recombinant proteins GST and GST-MKK5 were incubated with His-ILK5 or followed by GST-mediated pull-down. His-GFP protein was used as a negative control. proteins were detected using a-GST and a-His antibodies. **(C)** ILK5 interaction between MKK5 was demonstrated by split-luciferase imaging with/without ATP treatment. Split-luciferase imaging assay was performed after addition of 200 *μ*M ATP or MES buffer (pH 5.7) as a mock treatment in *N. benthamiana* leaves co-infiltrated with *GV3101* expressing MKK5-nLUC and ILK5-cLUC. Dotted circles indicate the infiltrated area in *N. benthamiana* leaves. MKK8-nLUC was used as a negative control. **(D)** Quantification of ILK5-MKK5 interaction signal intensities under ATP treatment. ILK5-MKK5 interaction was monitored, images were captured, and luciferase signal intensities were quantified using C-vision/Im32 and analyzed using the GraphPad Prism 8. Data shown as mean ± SEM, n = 7 (biological replicates), ****p<0.0001, ***p<0.001, **p<0.01, p-value indicates significance relative to MKK8-cLUC and was determined by unpaired two-tailed Student's t test. **(E)** MKK5 can be phosphorylated by purified from *N. benthamiana* recombinant ILK5 and His-ILK5^{S192A} protein displays reduced phosphorylation of MKK5^{K99R} protein *in vitro*. Purified from *N. benthamiana* recombinant His-ILK5 or His-ILK5^{S192A} recombinant protein were incubated with GST-His-MKK4^{K108R} or GST-His-MKK5^{K99R}, followed by an *in vitro* kinase assay. **(F)** ILK5 protein phosphorylates the MKK5 activation loop S/TxxxxxS/T motif. Protein purified from *N. benthamiana* recombinant His-ILK5 protein was incubated with GST-His-MKK5 kinase-dead (GST-His-MKK5^{K99R}) and GST-His-MKK5 triple mutation (GST-His-MKK5^{K99RT215AS221A}) or GST in an *in vitro* kinase assay. In panel E and F, autophosphorylation and trans-phosphorylation were detected by incorporation of γ-[^{32}P]-ATP. MBP was used as an universal substrate. Protein loading was visualized by CBB staining. **(G)** MKK5 phosphorylation is significantly reduced in *ilk5-1* mutant plants. MKK5-HA protein was expressed in wild-type and *ilk5-1* protoplasts with/without 250 *μ*M ATP treatment, then subjected to IP and IB using anti-HA and anti-phospho-Ser/Thr antibodies. Protein loading was visualized by CBB staining. All above experiments were repeated two times with similar results.

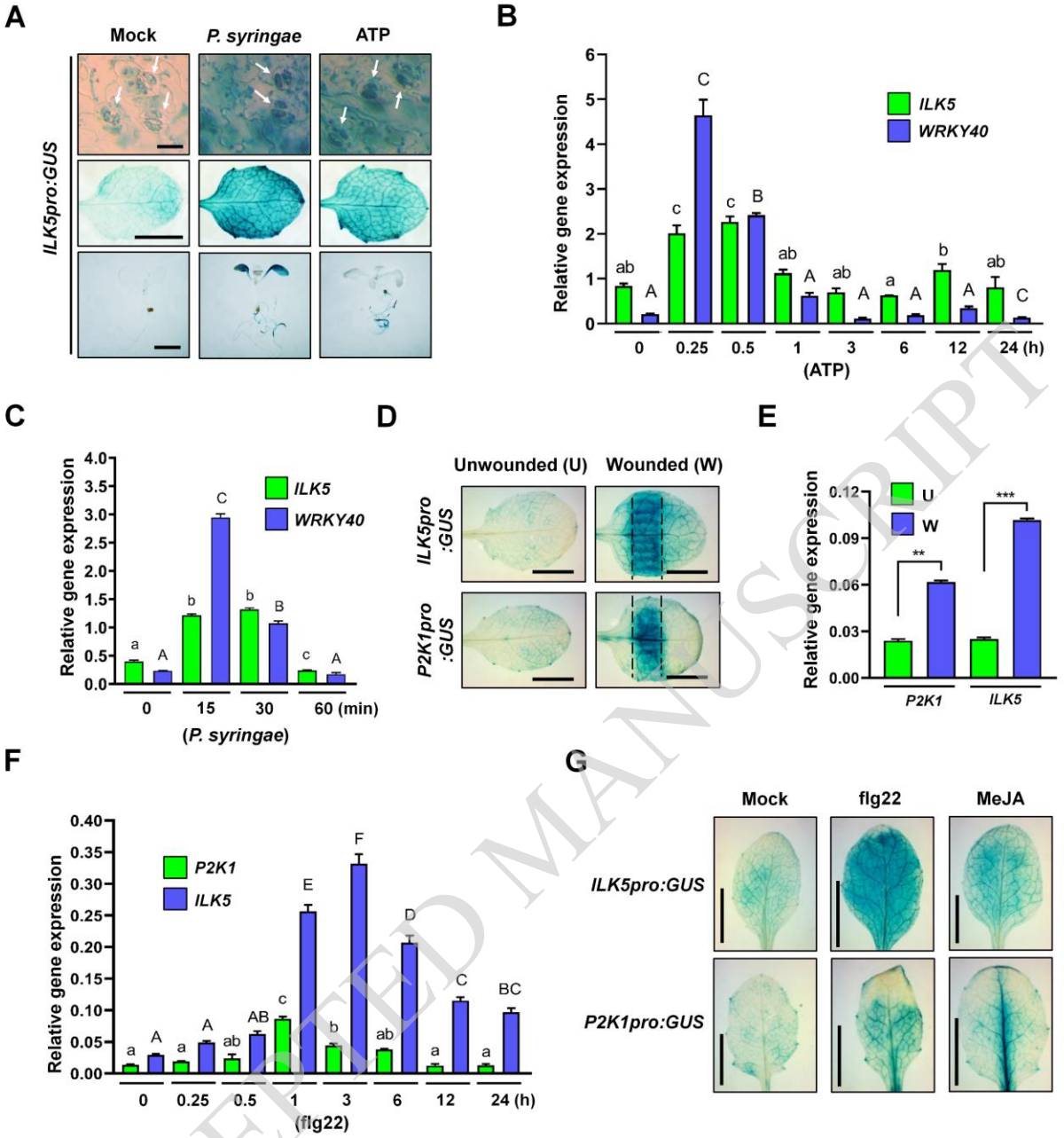

Figure 4. *ILK5* is highly induced after addition of ATP or *P. syringae* DC3000 inoculation. (A) Histochemical analysis of *ILK5* gene expression after ATP treatment or *P. syringae* DC3000 inoculation. *ILK5promoter:GUS* transgenic plants were constructed in wild-type Arabidopsis plants transformed with a chimeric *ILK5promoter:GUS* including 2 kb of the putative *ILK5* promoter (5′ region of the *ILK5* gene) fused to the *GUS* coding sequence. The expression patterns of the *ILK5promoter:GUS* transgenic plant was detected by histochemical staining in a 10 day-old seedling rosette leaf treated with 200 *μ*M ATP or inoculated with *P. syringae* DC3000 (OD_{600} = 0.05) after 1 hour. Arrows in upper panel indicate the stained guard cells. Scale bars = upper, 20 *μ*m; middle and bottom, 4 mm. (**B)** Reverse transcription quantitative-PCR (RT-qPCR) analysis of *ILK5* transcripts after ATP (200 *μ*M) treatment. **(C)** *ILK5* gene expression was measured by RT-qPCR analysis in response to *P. syringae* inoculation. In panel B and C, total RNA was isolated from 10-days old seeding plants at each time point and 2 *μ*g of total RNAs were used in this experiment. The *SAND* reference gene was used for data normalization. *WRKY40* was used as an inducible marker gene for the response to ATP treatment (n = 3) and *P. syringae* inoculation (n = 3). **(D)** Histochemical analysis of *ILK5promoter:GUS* and *P2K1promoter:GUS* expression in response to wounding. The expression patterns of the *ILK5promoter:GUS* and *P2K1promoter:GUS* transgenic plants were detected by histochemical staining of 2-week-old GUS transgenic plants after wounding. Scale bars = 4 mm. **(E)** RT-qPCR analysis of *ILK5* and *P2K1* gene expression in response to wounding. Data shown as mean ± SEM, n = 2 (biological replicates), ***p<0.001, ** p<0.01, p-value was determined and analyzed using the GraphPad Prism 8 by unpaired two-tailed Student's t test. **(F)** RT-qPCR analysis of *ILK5* and *P2K1* gene expression (n = 3) at different time points in response to flg22 treatment. The *SAND* reference gene was used for data normalization. **(G)** Histochemical analysis of 10-day-old seedling *ILK5promoter:GUS* and *P2K1promoter:GUS* in response to flg22 (100 nM) and MeJA (1 *μ*M). In panel B, C and F, data shown as mean ± SEM, Different letters above the bars indicates significant differences (p<0.05). p-value was determined and analyzed using the GraphPad Prism 8 by one-way ANOVA followed by Tukey's multiple comparisons. All above experiments were repeated two times (biological replicates) with similar results. Scale bars = 2 mm.

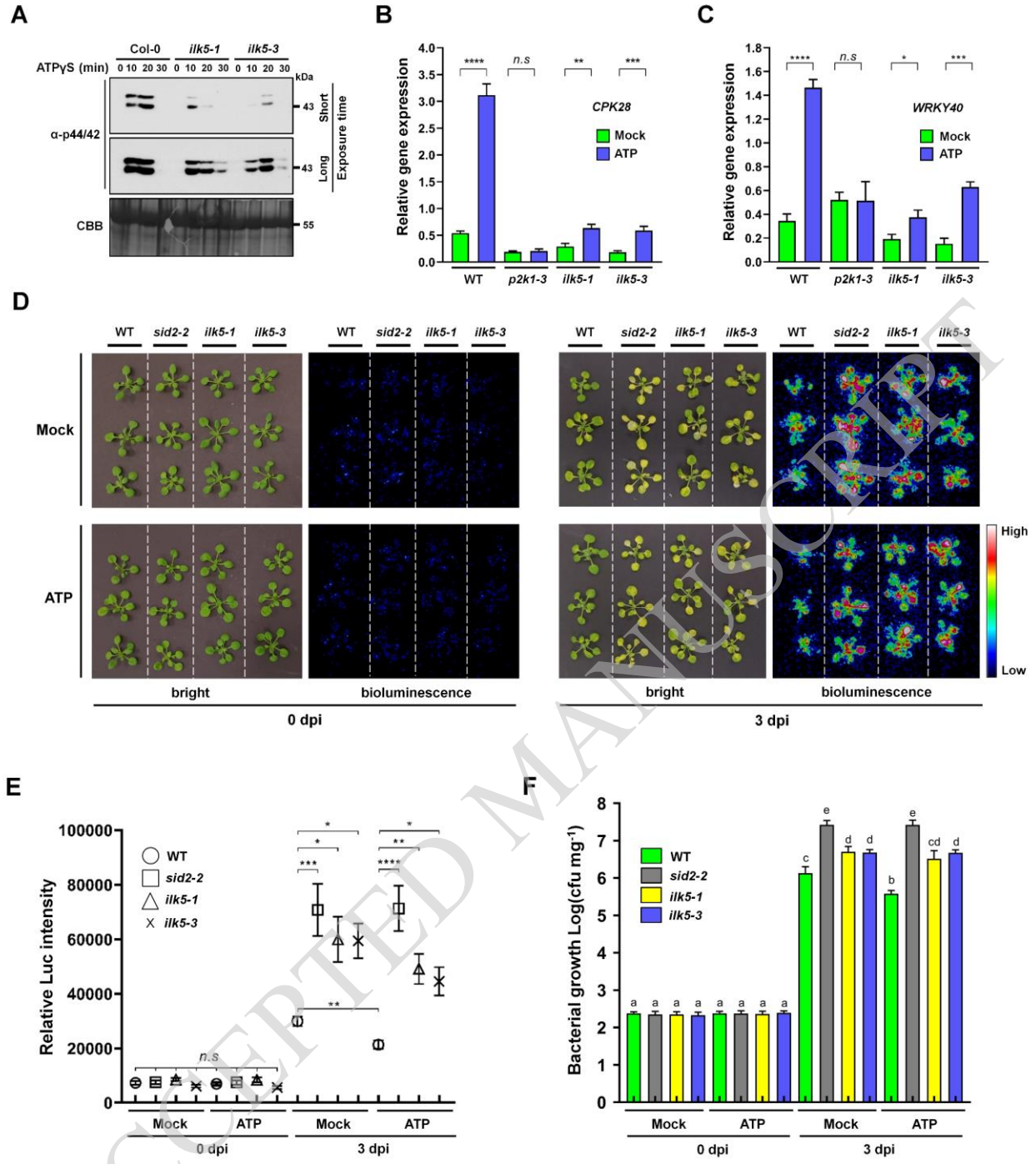

Figure 5. ILK5 is required for plant innate immunity. (A) Phosphorylation of MPK3/6 detected in *ilk5* mutants by immunoblotting using anti-phospho 44/42 antibody. ATPγS (250 *μ*M) was added and incubated for the times shown. Total protein was extracted at each time point and IB was performed with an anti-phospho 44/42 MAPK antibody. CBB staining of protein was used as a loading control. These experiments were repeated three times with similar results. **(B-C)** RT-qPCR analysis of *CPK28* and *WRKY40* transcripts in *p2k1-3, ilk5-1* and *ilk5-3* mutant backgrounds after ATP (250 *μ*M) treatment. Total RNA was isolated from 2 weeks-old plants and 2 *μ*g of total RNA was used in this experiment. The *SAND* reference gene was used for data normalization. Data shown as mean ± SEM, *WRKY40;* (n = 4), *CPK28;* (n = 6), ****p<0.0001, ***p<0.001, **p<0.01, *p<0.05, p-value indicates significance relative to mock treatment and was determined and analyzed using the GraphPad Prism 8 by unpaired two-tailed Student's *t* test. These experiments were repeated three times with similar results. (**D)** Three-week-old plants were flood inoculated with *luxCDABE*-tagged *P. syringae* DC3000 suspension (5×10^6 CFU mL^{-1}) containing 0.025% (v/v) Silwet L-77 with or without the addition of ATP (250 *μ*M). Bioluminescence was detected using a low light capture CCD camera at the time of inoculation (0 days) and 3 days post inoculation. **(E)** Quantification of bioluminescence signal intensities. The signal of *luxCDABE*-tagged *P. syringae* DC3000 was monitored, images were captured, and the luciferase signal intensities were quantified using the C-vision/Im32 program (n = 9). **(F)** Bacterial colonization was determined by plate counting (n = 8). In panel E and F, data shown as mean ± SEM, ****p<0.0001, ***p<0.001, **p<0.01, *p<0.05, p-value and different letters above the bars indicates significance relative to wild-type plants and was determined and analyzed using the GraphPad Prism 8 by two-way ANOVA followed by Tukey's multiple comparisons test. These experiments were repeated three times (biological replicates) with similar results.

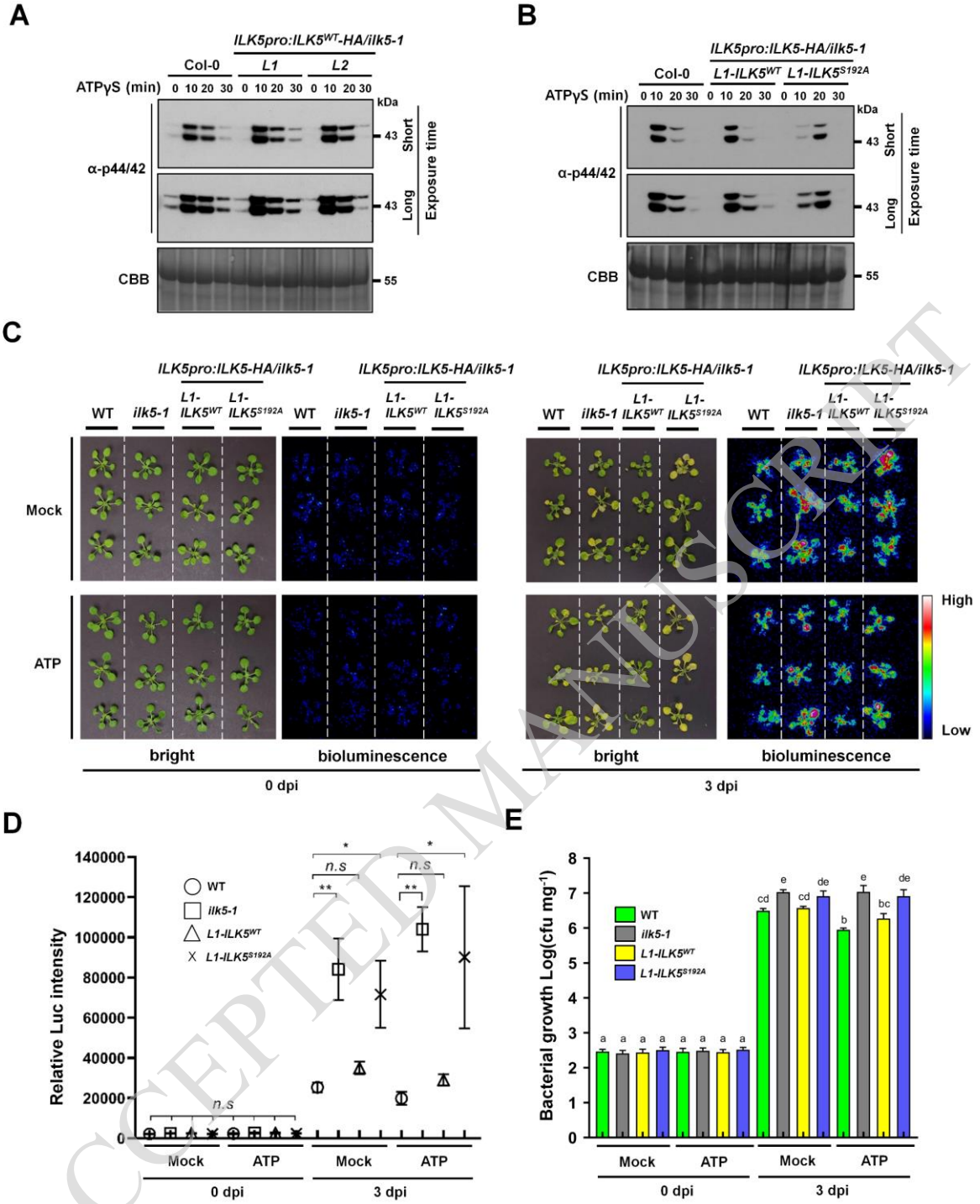

Figure 6. Expression of the ILK5^{S192A} mutant protein increases plant susceptibility to *P. syringae* infection. (A) Phosphorylation of MPK3/6 detected in complemented lines in which *ILK5* expression was driven by the native promoter (*L1* and *L2*) by immunoblotting using anti-phospho 44/42 antibody. ATPγS (250 *μ*M) was added and incubated for the times shown. **(B)** Phosphorylation of MPK3/6 was detected in complemented lines where the ILK5^{WT}or ILK5^{S192A} protein were expressed from the *ILK5* native promoter in *ilk5-1* mutant background (*L1-ILK5^{WT}* or *L1-ILK5^{S192A}*). Immunoblotting was performed using anti-phospho 44/42 antibody with 250 *μ*M ATP. In A and B, total protein was extracted at each time point after addition of 250 *μ*M ATP. CBB staining of protein was used as a loading control. These experiments were repeated three times with similar results. **(C)** Three-week-old plants were flood inoculated with *luxCDABE*-tagged *P. syringae* DC3000 suspension in the presence of 250 *μ*M ATP. Inoculated plants (Col-0, *ilk5-1*, *L1-ILK5^{WT}-HA*, or *L1-ILK5^{S192A}-HA complemented lines*), were used and bioluminescence was detected using a low light capture CCD camera either at the time of inoculation (0 day) and 3 days post inoculation. **(D)** Quantification of luminescence signal intensities. The signal of *luxCDABE*-tagged *P. syringae* DC3000 for each plant was monitored, images were captured, and the luciferase signal intensities were quantified using the C-vision/Im32 program. **(E)** Bacterial colonization was determined by plate counting. In panel C (n = 6) and D (n = 8), data shown as mean ± SEM, ****p<0.0001, ***p<0.001, **p<0.01, *p<0.05, p-value and different letters above the bars indicates significance relative to wild-type plants and was determined and analyzed using the GraphPad Prism 8 by two-way ANOVA followed by Tukey's multiple comparisons test. These experiments were repeated three times (biological replicates) with similar results.

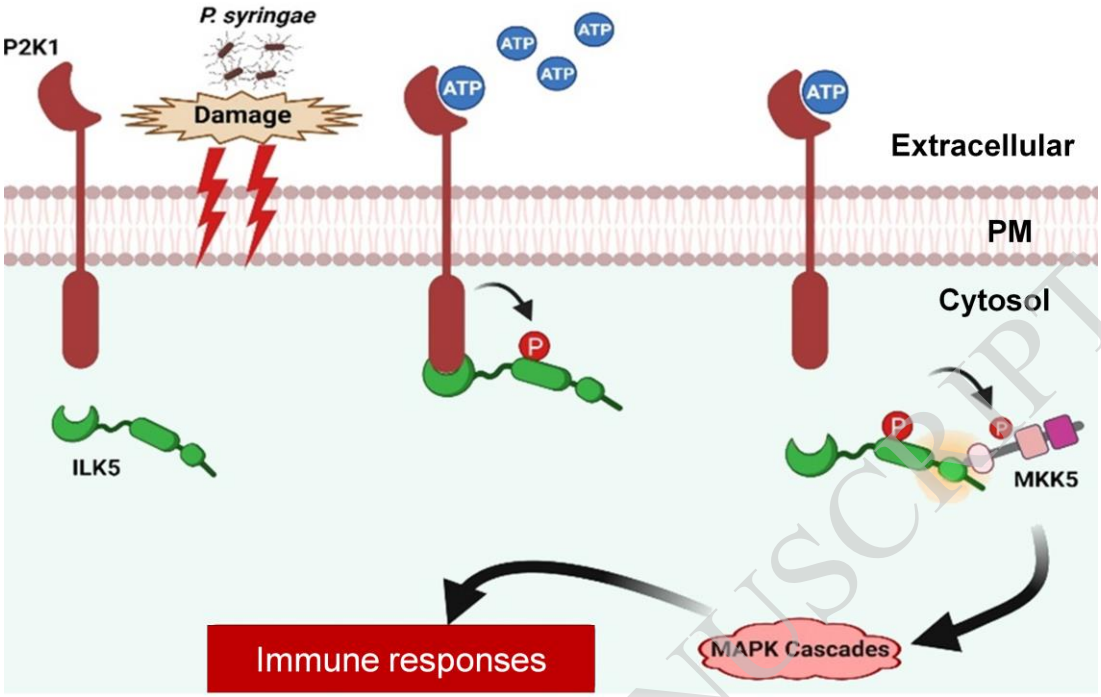

Figure 7. Hypothetical model for the role of ILK5 in eATP signaling. Upon addition of the activating ligand eATP, the P2K1 receptor is rapidly auto-phosphorylated and then directly interacts and phosphorylates its downstream target, the ILK5 protein, leading to pattern-triggered immune response via MAPK cascades.